Chapter 2

Polycyclic Fused Aromatic Pyrrole-based Conjugated Polymers

Table of Contents

Introduction

Since the past two decades, conjugated polymers have grabbed undivided attention of the researchers, as they can be simply and cost-effectively processed compared to their inorganic counterparts.[1,2] Another added advantage of these materials is possibility of having tunable electronic and optical properties *via* molecular engineering.[2] The key of this molecular engineering lies in controlling the π conjugation over the polymer backbone.[3] For many years, conjugated polymers having benzenoid or heterocyclic units like poly(*p*-phenylene), polyaniline, polythiophene and polypyrrole have been materials of choice for researchers as electrical conducting materials.[4]

The unsubstituted poly(*p*-phenylene) (**PPP**) is a structurally well-defined conjugated polymer prototype and it has been studied very well since a long time. In neutral form, **PPP** is an insulator, which becomes conducting (~500 Ω^{-1} cm^{-1}) up on doping.[5,6] **PPP** has become a promising candidate for applications in organic electronics in light of its significant properties like compressive strength, low density and high stability toward temperature, oxygen and moisture.[7] Polyaniline (**PANi**) is an another representative from the family of conducting polymers, which consists of monomer units built from reduced and oxidized blocks.[8] **PANi** and its composite materials have been widely used in energy storage and conversion devices, including supercapacitors, batteries and fuel cells.[9] **PANi** has garnered much attention, among the conducting polymers owing to its properties like highest specific capacitance due to the multi-redox reactions, good electronic properties due to the protonation, better thermal stability, low cost due to its infinite abundance and ease of synthesis (chemical or electrochemical methods) resulting in powder or thin films.[10,11] Apart from this, polythiophenes (**PTh**) have gained much attention due to their great capability to be integrated as light absorbing materials in organic electronic devices, over the last four decades. Polythiophenes are most well-known owing to its electrical conductivity, resulting from the electron delocalization along the polymer backbone. Moreover, these materials exhibit dramatic colour shifts in response to the changes in solvent (solvatochromism), temperature (thermochromism), applied potential (electrochromism) and binding to the other molecules.[12] Polythiophene polymers can be used as electrical conductors, recording materials, nonlinear optical devices, polymer light-emitting diodes, electrochromic or smart windows, photoresists,

antistatic coatings, sensors, batteries, electromagnetic shielding materials, artificial noses and muscles, solar cells, electrodes, microwave absorbing materials, new types of memory devices, transistors, nanoswitches, optical modulators and valves, imaging materials, polymer electronic interconnects, and nanoelectronic and optical devices.[13]

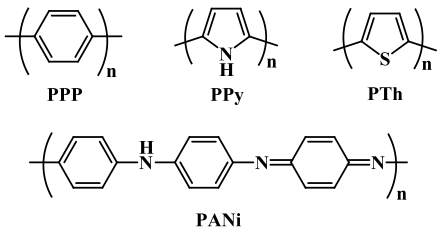

Figure 2.1 Structures of various class of conducting polymers

Among these materials, polypyrrole (**PPy**) exhibits promising candidature for many commercial applications like electronic devices, functional membranes, electrochromic windows and displays,[14–17] solid electrolytic capacitors, anti-electrostatic coatings, wires, microactuators, biosensors and gas sensors etc. because of its higher conductivity, facile synthesis and good environmental stability.[18] Polypyrrole films have remarkable influence in the field of molecular electronic devices, solid-state 'batteries' and chemically modified electrodes and sensors due to their solid-state properties.[19] These remarkable properties of polypyrrole comes from the pyrrole monomer, which has significantly lower oxidation potential than that of other five membered heterocyclic aromatic monomers, like thiophene and furan.[20] Apart from polypyrroles, researchers have utilized substituted pyrrole and pyrrole derivatives as monomers for various conjugated polymer synthesis involving 3-substituted ketopyrroles,[19] 3-substituted oligo(ethyleneoxy)pyrroles,[4] 2,5-di(2-thienyl)pyrroles,[21] bis(pyrrol-2-yl)arylenes,[20] *N*-alkyldithienopyrroles,[3] 1,2-di(3-pyrrolyl)benzene,[22] thiadiazole-fused thienopyrroles[23] etc.

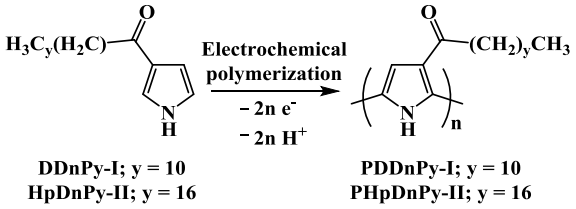

Figure 2.2 Electrochemical polymerization of 3-substituted ketopyrrole derivatives

Bryce *et al*. have reported electrochemical polymerization of 3-substituted ketopyrrole derivatives, 1-(1*H*-pyrrol-3-yl)dodecan-1-one (**DDnPy-I**) and 1-(1*H*-pyrrol-3-yl)heptadecan-1-one (**HpDnPy-II**), using tetra-*n*-butylammonium

hexafluorophosphate ($TBAPF_6$) and ITO as an anode. The polymers obtained *via* electrochemical polymerization (**PDDnPy-I** and **PHpDnPy-II**) exhibited high electrical conductivities of 360 S cm^{-1} and 10 S cm^{-1}, respectively.[19] Moon *et al.* reported monomeric pyrroles, **DHPy-I** and **TDPy-II**, derivatized at the 3-position with a poly(ethyleneoxy) group separated from the pyrrole ring by an ethylene group. These monomeric pyrroles were subjected to the electrochemical polymerization in the one compartment cell using lithium perchlorate as an electrolyte and the obtained polymers **PDHPy-I** and **PTDPy-II** exhibited high quality polymer films with electrical conductivity of 0.08 S cm^{-1} and 15 S cm^{-1}, respectively using a four point probe method.[4]

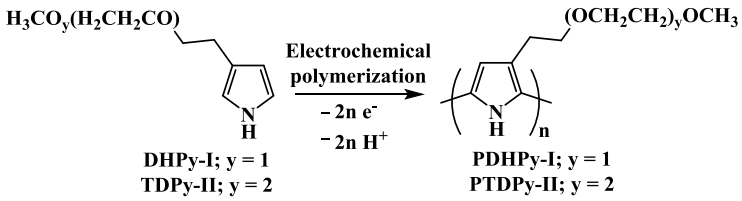

Figure 2.3 Electrochemical polymerization of 3-substituted oligo(ethyleneoxy)pyrrole derivatives

Wu *et al.*[21] have reported two dithienylpyrrole derivatives, **INDThPy** and **MDBDThPy**, which were subjected to the electrochemical polymerization to yield homopolymers , **PINDThPy** and **PMDBThPy**, and their copolymers with perylene, **P(INDThPy-co-Perylene)** and **P(MDBDThPy-co-Perylene)**.

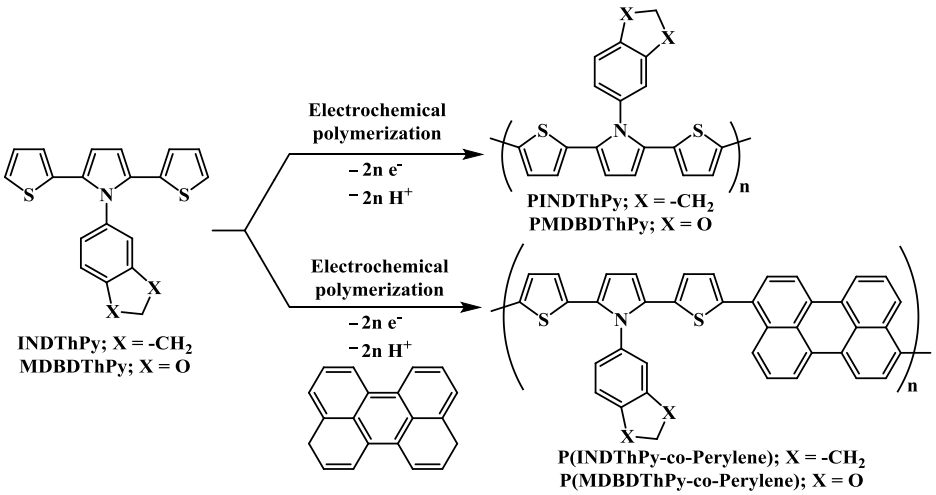

Figure 2.4 Electrochemical polymerization of dithienylpyrrole derivatives, **INDThPy** and **MDBDThPy**

These thienylpyrrole-based conducting polymer films were investigated for electrochromic properties in an ionic liquid solution, using spectroelectrochemistry,

switching and colouration efficiency. Spectroelectrochemistry suggested that these polymer films have distinct electrochromic properties from a yellow (or yellowish-green) colour in neutral state to blue colour in oxidized state with applied voltage.

Sotzing *et al.*[20] reported synthesis of bis(pyrrol-2-yl)arylenes (**BPB**, **BPB-OCH$_3$** and **BPBN**), having two pyrrole rings connected *via* 2-position to the different central arylene units and polymerized them successfully using electrochemical polymerization. These bis(pyrrol-2-yl)arylenes exhibit lower oxidation potential, which, in turn, help to limit the amount of side reactions (i.e., formation of *β*-linkages, over oxidation of polymers, etc.) during the electropolymerization. The synthesized electropolymers **PBPB**, **PBPB-OCH$_3$** and **PBPBN** exhibited moderate optical bandgaps ranging between 2.3 eV−2.4 eV and stability to multiple double-potential-step switchings, as required for eletrochromic devices and electromagnetic shutters.

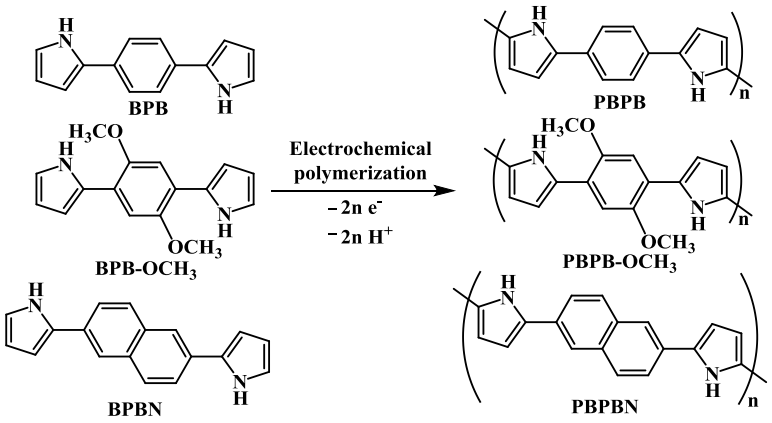

Figure 2.5 Electrochemical polymerization of bis(pyrrol-2-yl)arylene derivatives, **BPB**, **BPB-OCH$_3$** and **BPBN**

Liu *et al.*[3] reported a novel fused tricyclic *N*-alkyldithieno[3,2-*b*:2′,3′-*d*]pyrrole (**DTPC8** and **DTPC12**) monomers, having central *N*-alkylpyrrole ring fused with two thiophene units and copolymerized it with different alkylated thiophene (T) and bithiophene (2T) units *via* Stille polymerization. The obtained DTP-based copolymers **PDTPC8-*alt*-TC8**, **PDTPC8-*alt*-TC12**, **PDTPC12-*alt*-TC12** and **PDTPC8-*alt*-2TC12** showed low optical bandgaps ranging between 1.7 eV−1.9 eV and electrical conductivity of 95 S cm^{-1}, 82 S cm^{-1}, 233 S cm^{-1} and 68 S cm^{-1}, respectively for iodine doped samples. Moreover, copolymers **PDTPC12-*alt*-TC12** and **PDTPC8-*alt*-2TC12** exhibited the field effect performance with the average mobility of 0.026 cm^{2}V^{-1}s^{-1} and 0.13 cm^{2}V^{-1}s^{-1}, respectively for as cast polymer films under inert atmosphere. Nadeau *et al.*[22] reported *β*-linked dipyrrole monomers, 1,2-di(3-pyrrolyl)benzene (***o*-DPB**), 3,4-di(3-pyrrolyl)thiophene (**DPTh**) and 1,3-di(3-

pyrrolyl)benzene (***m*-DPB**), which can be subjected to the electrochemical polymerization to generate families of conducting polymers with selected functionality.

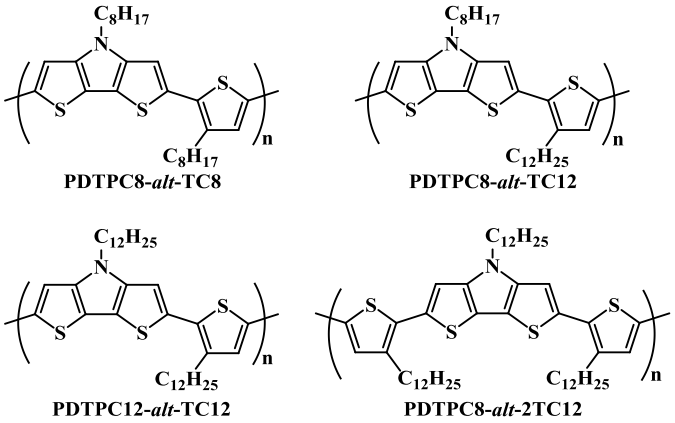

Figure 2.6 Structure of tricyclic fused *N*-alkyldithieno[3,2-*b*′:2,3-*d*′]pyrrole (**DTP**)-based copolymers **PDTPC8-*alt*-TC8, PDTPC8-*alt*-TC12, PDTPC12-*alt*-TC12** and **PDTPC8-*alt*-2TC12**

Out of the synthesized monomers, ***o*-DPB** exhibited electrochemical oxidation which leads to the intramolecular cyclization followed by the polymerization to give **Poly-I**, which was proven to be a robust conducting and electrochromic polymer with *in-situ* measured conductivity of 0.0038 S cm^{-1}–0.012 S cm^{-1} for **Poly-I** grown on Pt interdigitated microelectrodes (IMEs) and from the spectroelectrochemical studies. On the other hand, **DPTh** showed redox behaviour which is not as robust as that observed for ***o*-DPB**. The electropolymerization of **DPTh** leads to the poor polymer growth, owing to the possibility of incomplete intramolecular cyclization of the **DPTh** and competitive oxidative polymerization through the redox active thiophene, leading to the defects in the polymer backbone.

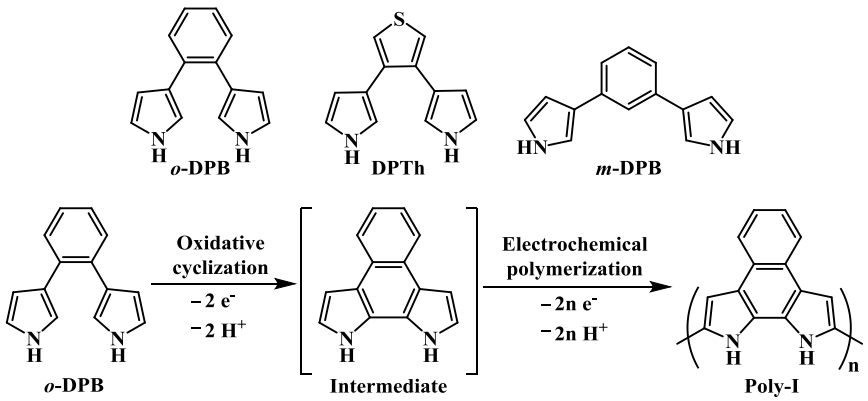

Figure 2.7 Structure of *β*-linked dipyrrole monomers, 1,2-di(3-pyrrolyl)benzene (***o*-DPB**), 3,4-di(3-pyrrolyl)thiophene (**DPTh**) and 1,3-di(3-pyrrolyl)benzene (***m*-DPB**) and electrochemical polymerization of ***o*-DPB** towards a robust electrochromic conducting **Poly-I**

Various strategies are adopted by researchers for synthesis of π conjugated polymers, out of which, three strategies are described below. One strategy is the synthesis of regio-regular polymer which leads to the defect-free, structurally homogeneous head-to-tail coupled polymer with enhanced π-conjugation, improved electronic and optical properties. Second strategy is the synthesis of alternative donor-acceptor system using various C-C coupling reactions. The third strategy is the introduction of fused aromatic rings into the conjugated polymer backbone, which is very useful to have polymers with high charge career mobility.[24,25] Fused rings help to achieve planar and more rigid polymer backbone, which in turn leads to enhanced effective π-conjugation, reduced chain-folding and lower band-gap. Moreover, rigid fused ring structure lowers the reorganization energy of the polymer, which facilitates intermolecular hoping and charge career mobility.[26,27] Many aromatic fused ring based conjugated polymers have been reported for the potential applications like organic light-emitting diodes (OLEDs), organic photovoltaic devices (OPVs) and field effect transistors (FETs).[3]

McCullough and co-workers used planar *N*-alkyldithienopyrroles as a fused aromatic building block and soluble substituted thiophenes for developing a series of novel electroactive and photoactive conjugated copolymers having a lower band-gap and higher conductivities.[3] Swager and co-workers reported the facile synthesis of fused polycyclic aromatic pyrrole based conjugated polymer from 1,2-di(3-pyrrolyl)benzene using tandem cyclisation/polymerization strategy. Resulting conjugated polymer poly(naphthobipyrrole) revealed a new class of robust, electrochromic conducting polymers having planarity and a good π-conjugation along the polymer backbone, derived from the aromatic fused ring structure.[22] We have synthesized a series of polycyclic fused aromatic pyrrole-based building blocks, benzodipyrrole (**BDP**), *N,N′*-dioctylbenzodipyrrole (**DOBDP**), *N,N′*-dioctyl-3-octylbenzodipyrrole (**TOBDP**), naphthobipyrrole (**NBP**) and *N,N′*-dioctylnaphthobipyrrole (**DONBP**) (Figure 2.8) and studied them electrochemically. These polycyclic fused aromatic pyrrole-based building blocks show preponderant reactivity at carbons 3 and 8 (i.e., the *β* and *β′*-pyrrolic positions) for electrophilic substitution.[28,29] Also, the research findings of Swager and co-workers have revealed reactivity of the α and α′-pyrrolic positions towards oxidative coupling reactions which

leads to the conjugated polymer.[22] Based on these findings, we have developed new naphthobipyrrole-based conjugated polymer.

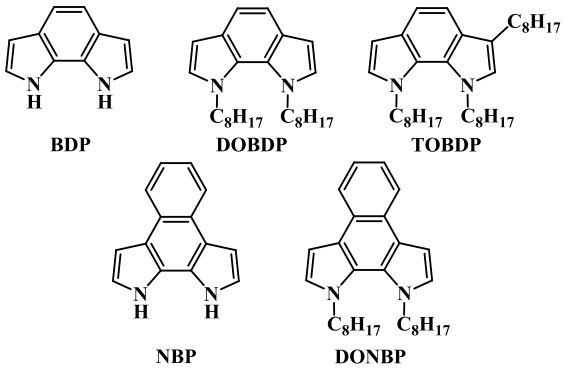

Figure 2.8 Synthesized polycyclic fused aromatic pyrrole-based monomers; **BDP**, **DOBDP**, **TOBDP**, **NBP** and **DONBP**[30]

Part-A: Synthesis, characterization and electrochemistry of monomers

Results and discussion

Synthesis of polycyclic fused aromatic pyrrole-based monomers

The tricyclic aromatic monomer, having peripheral pyrrole rings fused to the central benzene ring, 1,8-dihydropyrrolo[3,2-*g*]indole (**BDP**) was synthesized as shown in Scheme 2.1. This compound was first reported by Berlin *et al*.[31] Modified synthesis of the same compound was reported by Clentsmith *et al*. using the strategy Rh(I)-catalyzed hydroamination and intramolecular cyclization of ortho-alkynylanilines to yield benzo(dipyrroles).[32] We hereby report tetra-*n*-butylammoniumfluoride (TBAF)-mediated intramolecular cyclization of ortho-alkynylacetanilide (*N,N′*-(3,6-bis((trimethylsilyl)ethynyl)-1,2-phenylene)diacetamide, compound **5**). Compounds **1**, **2** and **3** were synthesized according to the literature.[33,34] Compound **4** was synthesized according to the method reported by Lindner *et al*.[35] Compound **5** was synthesized by *N*-acylation reaction of compound **4** using acetyl chloride and sodium bicarbonate as a mild base in dry diethyl ether at 0 ^{o}C. 1,8-dihydropyrrolo[3,2-*g*]indole (**BDP**) was synthesized from compound **5** using modification of literature procedure reported by Yasuhara *et al*.[36] TBAF mediated cyclization of compound **5** proceeded well in refluxing THF with 63% yield. The synthesized 1,8-dihydropyrrolo[3,2-*g*]indole (**BDP**), being an air-sensitive, was purified *via* flash column over silica gel using chloroform as eluent. The 1,8-dioctyl-1,8-dihydropyrrolo[3,2-*g*]indole (**DOBDP**) and 1,3,8-trioctyl-1,8-dihydropyrrolo[3,2-*g*]indole (**TOBDP**) were synthesized by alkylation reaction of **BDP** using excess of *n*-octylbromide and NaOH in DMF at 80 ^{o}C for 3 h. Both the **DOBDP** and **TOBDP** are being formed during the alkylation reaction. Formation of **TOBDP** along with **DOBDP** can be explained on the basis of the affinity of β and β'-pyrrolic positions towards electrophilic substitution reactions. Both the compounds were separated using column chromatography over silica gel using pet-ether as eluent.

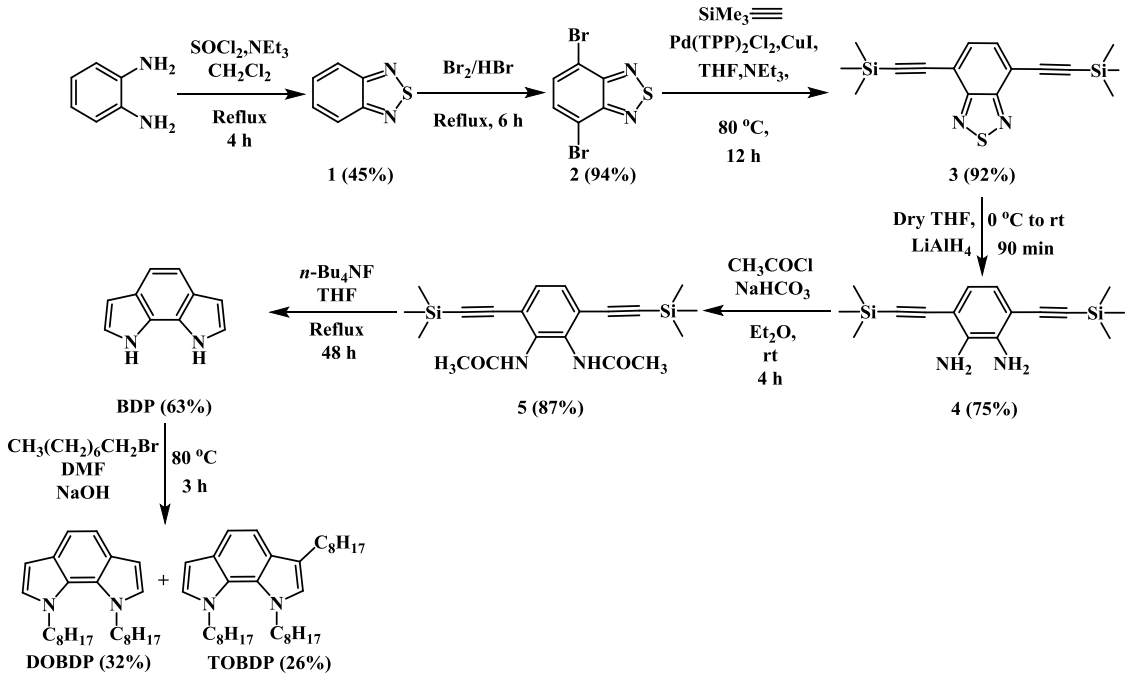

Scheme 2.1 Synthesis of polycyclic fused aromatic pyrrole-based **BDP**, alkylated **DOBDP** and **TOBDP** from 1,2-phenylenediamine[30]

The naphthalene analogue of **BDP**, 1,10-dihydrobenzo[*e*]pyrrolo[3,2-*g*]indole (**NBP**) is a known compound[37] and was synthesized as shown in Scheme 2.2 using literature procedure reported by Roznyatovskiy *et al*.[38] Compound **6** was synthesized according to the literature procedure reported by Franzen *et al*.[39] Compound **7** and **8** were prepared according to the literature procedure reported by Roznyatovskiy *et al*.[38] 1,10-dihydrobenzo[*e*]pyrrolo[3,2-*g*]indole (**NBP**) was synthesized using modification of the procedure reported by Roznyatovskiy *et al*.[38] from compound **8** using KOH as a base for hydroxylation of ethylester followed by de-carboxylation at elevated temperature in ethylene glycol under nitrogen atmosphere for 3 h. Crude product was obtained by filtration of the precipitates formed after quenching reaction mixture with de-ionized water. Crude product was subjected to column chromatography over silica gel using 40% ethyl acetate-petroleum ether system as eluent giving pure **NBP** in 60% yield. 1,10-dioctyl-1,10-dihydrobenzo[*e*]pyrrolo[3,2-*g*]indole (**DONBP**) was synthesized by *N*-alkylation reaction of **NBP** using excess of *n*-octylbromide and NaOH in DMF at 80 °C for 3 h. Pure compound **DONBP** was achieved in 75% yield by subjecting crude compound to column chromatography over silica gel using 1% ethyl acetate-petroleum ether system as eluent.

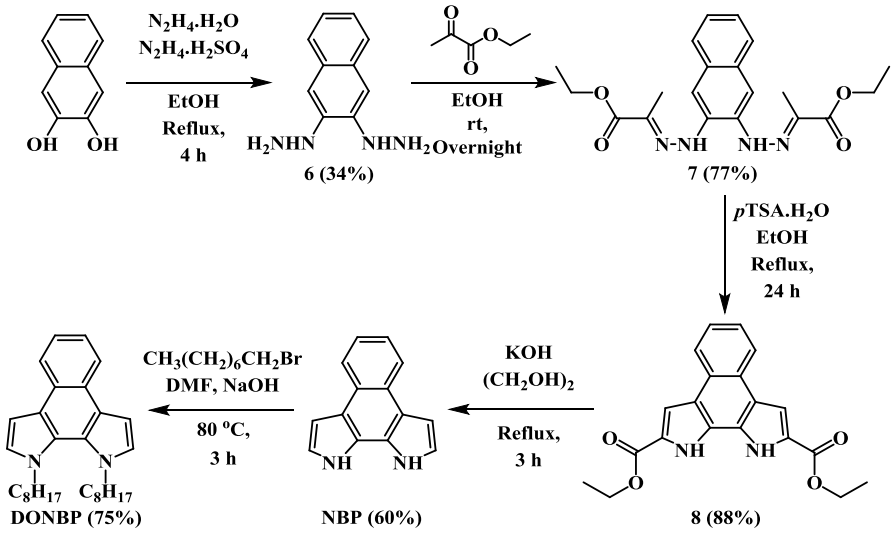

Scheme 2.2 Synthesis of polycyclic fused aromatic pyrrole-based **NBP** and alkylated **DONBP** from 1,2-dihydroxynaphthalene[30]

Characterization of the synthesized polycyclic fused aromatic pyrrole-based monomers

The synthesized tricyclic fused aromatic pyrrole-based compound **BDP** and its alkylated products **DOBDP** and **TOBDP** are characterized by ^{1}H and ^{13}C NMR spectroscopy, ESI-Mass spectroscopy and APCI-Mass spectroscopy. The tricyclic product 1,8-dihydropyrrolo[3,2-*g*]indole (**BDP**), obtained by the TBAF-mediated cyclization reaction of compound **5** in DMF/ chloroform, was characterized by ^{1}H and ^{13}C NMR spectroscopy and ESI-Mass spectroscopy.

Electrochemical properties of the synthesized polycyclic fused aromatic pyrrole-based monomers

The redox properties of the synthesized tricyclic fused pyrrole-based **BDP**, **DOBDP** and **TOBDP** and tetracyclic fused pyrrole-based **NBP** and **DONBP**, were studied by cyclic-voltammetry (CV). The CV experiments were performed in the dry acetonitrile solution of monomers (~ 5 mM) and $TBAPF_6$ as a supporting electrolyte (~ 50 mM) using three electrodes system: Pt disc electrode as working electrode, Pt wire electrode as counter electrode and Ag/Ag^{+} as a reference electrode. All monomers showed irreversible oxidation waves in cyclic voltammogram.

The cyclic voltammogram of **BDP** is shown in Figure 2.9a. BDP showed two irreversible oxidations, having anodic peak potential +1.22 V and +1.95 V, respectively. The HOMO energy level for **BDP** was calculated from the onset of first

oxidation peak at +0.78 V and the calculated E_{HOMO} value for **BDP** is −5.22 eV. The cyclic voltammogram of *N*-alkylated **DOBDP**, as shown in Figure 2.9b, exhibited one oxidation peak at anodic peak potential +0.86 V, with an oxidation onset potential +0.71 V. respectively and two reduction waves showing cathodic peak potential −1.08 V and −2.54 V, respectively when scanned between +2.50 V to −3.00 V at the scan rate of 50 mV/s. The first oxidation wave and the first reduction wave are quasi-reversible in nature. The HOMO level of **DOBDP** resides at −5.15 eV which is calculated from the onset of the oxidation peak. As shown in the Figure 2.9c, the cyclic voltammogram of trialkylated **TOBDP** is showing one irreversible oxidation peak, with anodic peak potential +0.74 V. The value of E_{HOMO} for **TOBDP** is −5.07 eV, which is calculated from the onset of the oxidation peak +0.63 V.

The cyclic voltammogram of tetracyclic fused pyrrole-based **NBP**, as per Figure 2.10a, shows irreversible oxidation at anodic peak potential +0.70 V with the onset oxidation potential of +0.55 V. The HOMO energy level of NBP was calculated from the onset oxidation potential and was found to be at −4.99 eV. The cyclic voltammogram of the *N*-alkylated **DONBP** (Figure 2.10b) exhibited irreversible oxidation with anodic peak potential of +0.72 V and the onset oxidation potential of +0.60 V. The value of the frontier orbital energy level, E_{HOMO}, was calculated from the onset of the oxidation wave and was found to be at −5.04 eV.

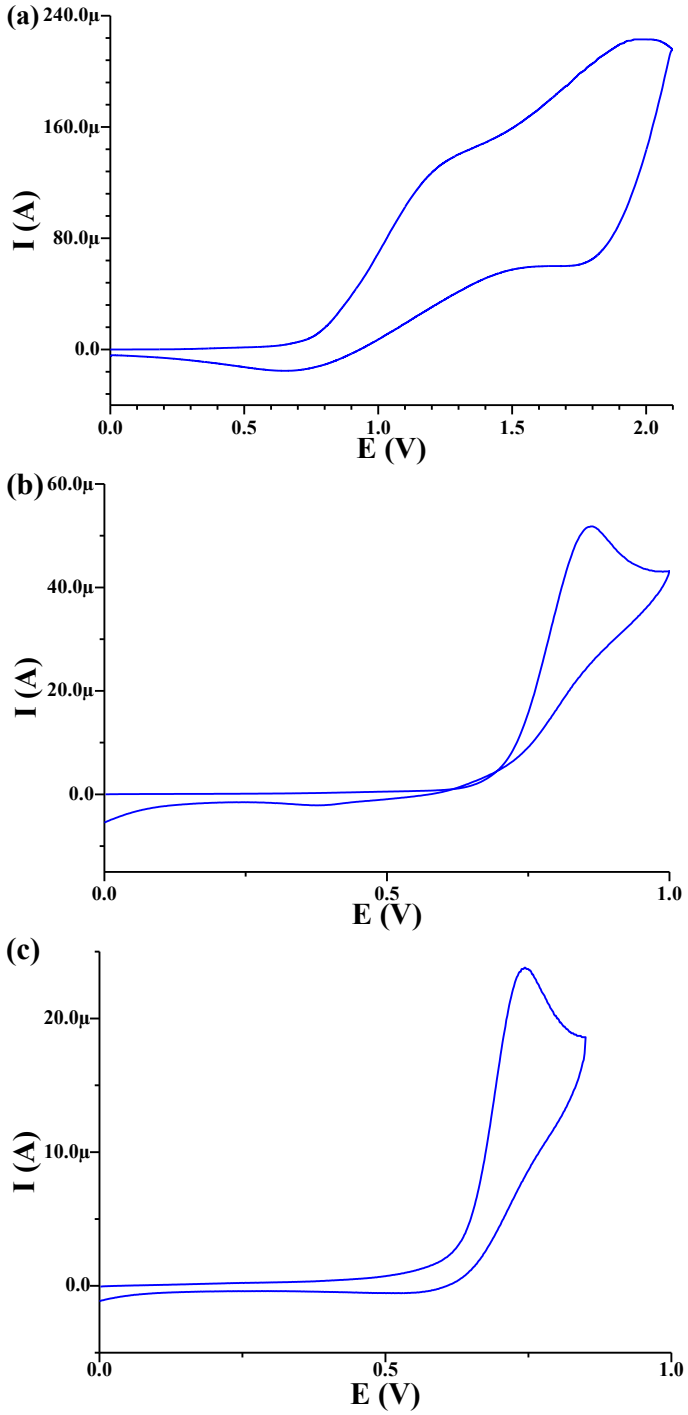

Figure 2.9 Cyclic voltammetry of (a) **BDP**; (b) **DOBDP** and (c) **TOBDP**, in acetonitrile (~5 mM) using $TBAPF_6$ as supporting electrolyte (~50 mM) cycled at 50 mV/s on Pt disc electrode; $E_{onset\ (Fc/Fc+)}$ = 0.36 V

It was noticed that the introduction of alkyl substituents onto the BDP-scaffold elevated the HOMO energy levels, in the order of E_{HOMO} (**TOBDP**) > E_{HOMO} (**DOBDP**) > E_{HOMO} (**BDP**), while in the case of the tetracyclic NBP-scaffold, introduction of the alkyl substituents lowered the HOMO energy level, in the order of E_{HOMO} (**NBP**) > E_{HOMO} (**DONBP**).

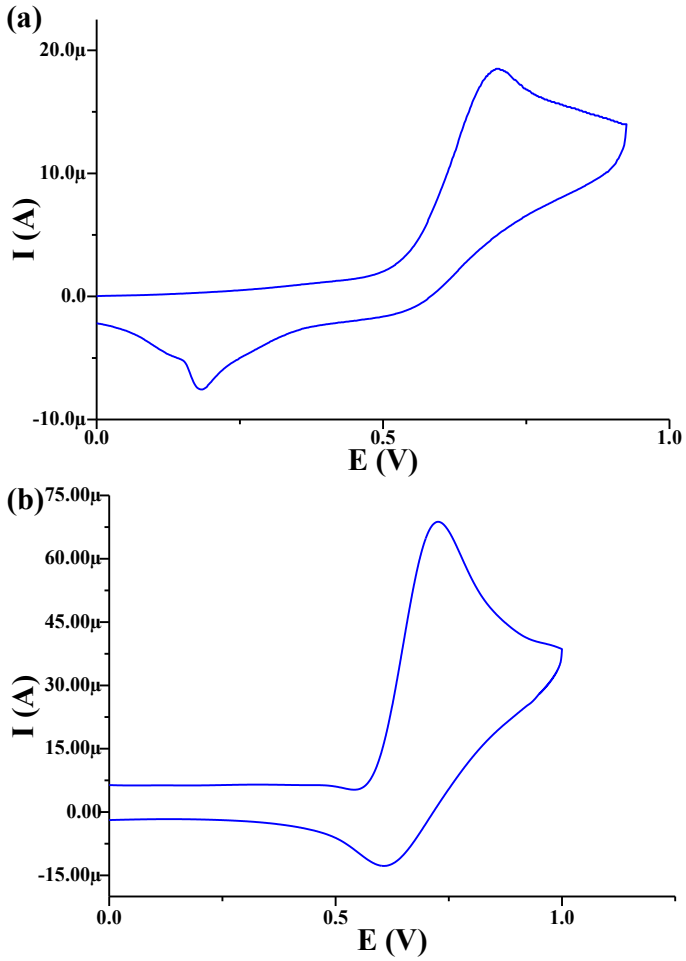

Figure 2.10 Cyclic voltammetry of (a) N**BP** and (b) **DONBP**, in acetonitrile (~5 mM) using $TBAPF_6$ as supporting electrolyte (~50 mM) cycled at 50 mV/s on Pt disc electrode; $E_{onset\ (Fc/Fc+)} = 0.36$ V

Table 2.1 Electrochemical properties of synthesized monomers; [a] potential v/s Ag/Ag^+; [b] calculated from equation $E_{HOMO} = -(E_{oxi,onset} + 4.8 - E_{onset\ (Fc/Fc+)})$.

Compound	E_{oxi} [a] (V)	$E_{oxi,onset}$ [a] (V)	E_{HOMO} [b] (eV)
BDP	+ 1.22	+ 0.78	− 5.22
DOBDP	+ 0.86	+ 0.71	− 5.15
TOBDP	+ 0.74	+ 0.63	− 5.07
NBP	+ 0.70	+ 0.55	− 4.99
DONBP	+ 0.72	+ 0.60	− 5.04

Conclusion

We have successfully synthesized five polycyclic fused aromatic pyrrole-based monomers, namely **BDP**, **DOBDP**, **TOBDP**, **NBP** and **DONBP**. The synthesized monomers showed moderate to good solubilities in common organic solvents like

dichloromethane, chloroform, ethyl acetate, THF, acetonitrile, etc. These monomers were characterized using ^{1}H NMR, ^{13}C NMR, ESI-Mass and APCI-Mass spectroscopy techniques. The synthesized monomers were studied electrochemically using cyclic voltammetry and the corresponding HOMO energy levels were calculated using the onset oxidation potentials obtained from the CV data of the monomers. Also, the effect of the introduction of the alkyl substituent onto the BDP- and NBP-scaffolds was studied, which revealed that the introduction of *n*-octyl chains on the BDP-scaffold elevated the HOMO energy levels while the introduction of *n*-octyl chains on the NBP-scaffold lowered the HOMO energy levels. In all of the synthesized monomers, **NBP** was found to be the most stable and electro-active monomer towards electro-chemical polymerization, considering its elevated HOMO energy level.

Experimental procedures

General procedures

All the chemicals were reagent grade and used as purchased. Moisture-sensitive reactions were performed under an inert atmosphere of dry nitrogen with dried solvents. Reactions were monitored by thin-layer chromatography (TLC) using Merck 60 F_{254} aluminium-coated plates and the spots were visualized under ultraviolet (UV) light. Column chromatography was carried out on silica gel (60–120 mesh). NMR spectra were recorded on a Bruker Avance-III 400 spectrometer in $CDCl_3$ and DMSO-D_6. Mass spectra were recorded on a Thermo-Fischer DSQ II GCMS instrument. CV data were obtained with CH Instruments model of CHI 600C with three electrode (Pt disc as the working electrode, platinum wire as the counter electrode, and non-aqueous $Ag/AgNO_3$ as the reference electrode) cell in anhydrous acetonitrile solution containing 50 mM tetra-*n*-butylammonium hexafluorophosphate ($TBAPF_6$) at a scan rate of 50 mV/s under an N_2 atmosphere. The redox onset potential of ferrocene/ferrocene^{+} ($E_{onset\ (Fc/Fc+)}$) under the same conditions is recorded. The HOMO levels were calculated by using the equation: $E_{HOMO} = -(E_{oxi,onset} + 4.8 - E_{onset\ (Fc/Fc+)})$.

Synthesis of tricyclic fused aromatic pyrrole-based monomers

The tricyclic fused aromatic pyrrole-based monomer, 1,8-dihydropyrrolo[3,2-*g*]indole (**BDP**), was synthesized using modification of literature procedure reported by Yasuhara *et al.*[36] by TBAF mediated intramolecular cyclization of ortho-alkynylacetanilides. Compounds **1** and **2** were synthesized according to the literature

procedures reported by Neto *et al*.[33] Compound **3** was synthesized according to the method reported by Appleton *et al*.[34] Compound **4** was synthesized according to the method reported by Lindner *et al*.[35]

Synthesis of 2,1,3-benzothiadiazole, **1**: To a 1000 mL round bottom flask were added 1,2-phenylenediamine (10.00 g, 92.47 mmol), 300 mL of dichloromethane and triethylamine (37.44 g, 369.98 mmol). The solution was stirred until total dissolution of the 1,2-phenylenediamine. To this stirred reaction mixture, a solution of $SOCl_2$ in small amount of dichloromethane was added very slowly and the resulting reaction mixture was refluxed for 4 h. The solvent was removed in a rotary evaporator and resulting concentrate was diluted with 700 mL of water. The final pH of the solution was adjusted to 2 by adding concentrated HCl. The desired compound was purified by direct steam distillation following addition of water to the mixture. The steam distilled mixture was extracted three times with 200 mL of dichloromethane, dried over MgSO4 and filtered. The solvent was removed, affording pure compound **1**.

2,1,3-benzothiadiazole, **1**: White solid (5.6 g, 45%); ^{1}H NMR (400 MHz, $CDCl_3$): 8.00−8.05 (dd, J_1 = 6.8 Hz, J_2 = 3.2 Hz, 1H), 7.59−7.63 (dd, J_1 = 6.8 Hz, J_2 = 3.2 Hz, 1H). ESI-Mass 135.90 [M+] (100.0%), 135.17 [M−1(-H)] (42.4%).

Synthesis of 4,7-dibromo-2,1,3-benzothiadiazole, **2**: To a 500 mL two-necked round bottom flask were added 2,1,3-benzothiadiazole, **1** (10.00 g, 73.44 mmol) and 150 mL of HBr (47%) and were allowed to stir at 60 ^{o}C for 15 min. A solution containing Br_2 (35.21 g, 220.32 mmol) in 100 mL of HBr was added dropwise to the reaction mixture. After addition of the Br_2, the resulting reaction mixture was refluxed for 6 h during which, precipitation of orange solid was observed. The mixture was allowed to cool to room temperature and un-reacted Br_2 was quenched by addition of saturated solution of $NaHSO_3$. The mixture was filtered under vacuum and washed exhaustively with water. The solid was then washed once with cold diethylether and dried under vacuum, affording the compound **2** in 95% yield (20.51 g, 69.77 mmol).

4,7-dibromo-2,1,3-benzothiadiazole, **2**: Off-white solid (20.3 g, 94%); ^{1}H NMR (400 MHz, $CDCl_3$): 7.75 (s, 1H). ESI-Mass 293.39 [M+] (100.0%), 291.39 [M−2] (50.2%).

Synthesis of 4,7-bis((trimethylsilyl)ethynyl)-2,1,3-benzothiadiazole, **3**: To an oven-dried 100 mL two-necked round bottom flask was added dry THF (20 mL) and triethylamine (20 mL), which was then vacuum degassed three times. 4,7-dibromo-

2,1,3-benzothiadiazole, **2** (1.43 g, 4.86 mmol), trimethylsilylacetylene (2.13 mL, 15.0 mmol), copper(I) iodide (9.26 mg, 0.05 mmol), and $Pd(PPh_3)_2Cl_2$ (35.1 mg, 0.05 mmol) were added to the flask under nitrogen atmosphere at room temperature. The reaction mixture was heated to 60 °C for 12 h under nitrogen atmosphere. After completion, the reaction was cooled to room temperature and 200 mL of water was added to the mixture and the aqueous solution was extracted with dichloromethane (2 X 100 mL). The combined organic layers were washed with water (3 X 200 mL), dried with magnesium sulfate, filtered, and dried in vacuo. The residue was purified by column chromatography on silica gel using pure hexane to afford compound **3**.

4,7-bis((trimethylsilyl)ethynyl)-2,1,3-benzothiadiazole, **3**: Bright yellow solid (1.5 g, 92%); ^{1}H NMR (400 MHz, $CDCl_3$): 7.72 (s, 1H), 0.35 (s, 9H). ESI-Mass 327.59 [M−1(-H)] (62.2%), 312.65 [M−(-CH_3)] (100.0%).

Synthesis of 3,6-bis((trimethylsilyl)ethynyl)benzene-1,2-diamine, **4**: The 4,7-bis((trimethylsilyl)ethynyl)-2,1,3-benzothiadiazole, **3** (0.10 g, 0.304 mmol) was dissolved in 10 mL of dry THF in a oven dried two-necked round bottom flask under nitrogen atmosphere. $LiAlH_4$ (0.058 g, 1.52 mmol) was added slowly over 5 min at 0 °C and resultant reaction mixture was kept stirring for 90 min at room temperature. After completion, the reaction mixture was again cooled down to 0 °C and quenched with a saturated NH_4Cl solution. The mixture was diluted with 30 mL of water and extracted with ethylacetate (3 X 30 mL). The combined organic layers were dried over anhydrous sodium sulphate and evaporated to dryness under vacuum. The crude product was purified by flash column chromatography over silica gel using 5% ethylacetate-petroleum ether as an eluent to afford orange brown air-sensitive compound **4**.

3,6-bis((trimethylsilyl)ethynyl)benzene-1,2-diamine, **4**: Orange brown solid (0.069 g, 75%); ^{1}H NMR (400 MHz, $CDCl_3$): 6.80 (s, 1H), 3.96 (br s, 2H), 0.28 (s, 9H).

Synthesis of *N,N'*-(3,6-bis((trimethylsilyl)ethynyl)-1,2-phenylene)diacetamide, **5**: The crude 1,4-diamino-2,5-bis(trimethylsilylethynyl)benzene, **4** (1.00 g, 3.32 mmol) was dissolved in 20 mL of dry diethyl ether. To this was added anhydrous sodium bicarbonate (1.40 g, 16.64 mol) and the resulting suspension was stirred at 0 ^{o}C for 10 min. To this cooled suspension, acetyl chloride (0.785 g, 9.98 mmol) was added drop wise, over a period of 5 min. After the complete addition, the reaction mixture was

stirred for 4 h at room temperature and quenched with water (30 mL). Organic layer was separated and aqueous layer was again extracted with dichloromethane (2 X 50 mL). Combined organic layer is washed with saturated brine solution, water, dried over anhydrous $MgSO_4$ and evaporated to dryness to yield pale yellow powder. Further purification was achieved by washing crude product with copious amounts of *n*-hexane, yielding white product.

N,N'-(3,6-Bis((trimethylsilyl)ethynyl)-1,2-phenylene)diacetamide, **5**: White solid (1.11 g, 87%); ^{1}H NMR (400 MHz, $CDCl_3$): 7.91 (s, 2H), 7.35 (s, 2H), 2.20 (s, 3H), 0.27 (s, 9H). ESI-Mass 384.04 [M+] (62%), 325.22 [M−(-$NHCOCH_3$)] (30%).

Synthesis of 1,8-dihydropyrrolo[3,2-*g*]indole (**BDP**): 1,8-dihydropyrrolo[3,2-*g*]indole (**BDP**) was synthesized using modified literature procedure as reported by *Yasuhara et al.*[36] *N,N'*-(3,6-bis(trimethylsilylethynyl)-1,2-phenylene)diacetamide, **5** (1.00 g, 2.6 mmol) was dissolved in 20 mL of dry THF in a flame dried two necked round bottom flask. To this stirred solution, TBAF (3.40 g, 13.00 mmol) (1 M in THF) solution (13 mL) was added drop wise, over a period of 5 min. After complete addition, the reaction mixture was refluxed for 48 h and monitored by TLC. After completion of the reaction, as indicated by TLC, 100 mL of water was added to it and extracted with aliquots of dichloromethane (2 X 50 mL). Combined organic layers are washed with saturated brine solution, water and dried over $MgSO_4$. Crude product is obtained after evaporation of solvent and subsequently subjected to *N*-alkylation as free form of 1,8-dihydropyrrolo[3,2-*g*]indole (**BDP**) is unstable and prone to blackening upon aerial oxidation.

1,8-Dihydropyrrolo[3,2-g]indole (**BDP**): Off-white solid (0.26 g, 63%); ^{1}H NMR (400 MHz, $CDCl_3$): 7.91 (s, 1H), 7.42 (s, 1H), 6.99−7.00 (dd, J_1 = 2.8 Hz; J_2 = 2.4 Hz, 1H), 6.65−6.67 (dd, J_1 = 3.2 Hz; J_2 = 2.4 Hz, 1H). ^{13}C NMR (100 MHz, CDCl3): 123.3, 122.0, 121.7, 113.8, 103.4. ESI-Mass 156.1 [M+] (100.0%), 154.7 [M−2(-H)] (93.6%).

Synthesis of 1,8-dioctyl-1,8-dihydropyrrolo[3,2-*g*]indole (**DOBDP**) and 1,3,8-trioctyl-1,8-dihydropyrrolo[3,2-*g*]indole (**TOBDP**): The **DOBDP** and **TOBDP** were synthesized as below. The crude **BDP** (1.64 g, 10.51 mmol) was dissolved in DMF (50 mL). To this, sodium hydroxide flakes (4.20 g, 105.12 mmol) was added and the resulting suspension was stirred at room temperature for 10 min. To this stirred solution, *n*-octylbromide (13.19 g, 68.33 mmol) was added dropwise, over a period of 5

min. After the complete addition, reaction mixture was stirred at 80 ^{o}C for 3 h and monitored by TLC. After completion of the reaction, as indicated by TLC, 200 mL of water was added to it and extracted with aliquots of dichloromethane (2 X 50 mL). Combined organic layers are washed with saturated brine solution, water and dried over anhydrous $MgSO_4$. Crude product is obtained after evaporation of solvent which is subjected to the column chromatography over silica gel using petroleum ether as an eluent. Both the **DOBDP** and **TOBDP**, being formed during the alkylation reaction are separated by column chromatography, yielding **TOBDP** as pinkish yellow oil from the initial fractions followed by **DOBDP** as yellow oil in the later fractions from the column.

1,8-Dioctyl-1,8-dihydropyrrolo[3,2-g]indole (**DOBDP**): yellow oil (1.28 g, 32%); ^{1}H NMR (400 MHz, $CDCl_3$): 7.35 (s, 1H), 6.99−7.00 (d, J = 2.8 Hz, 1H), 6.60−6.61 (d, J = 2.8 Hz, 1H), 4.32-4.36 (t, J = 7.6 Hz, 2H), 1.82−1.88 (m, 2H), 1.24−1.30 (m, 10H), 0.86-0.89 (t, J = 6.8 Hz, 3H). ^{13}C NMR (100 MHz, CDCl3): 127.6, 126.9, 124.2, 114.3, 103.6, 50.9, 31.7, 31.2, 29.2, 29.1, 26.8, 22.6, 14.1. APCI-Mass 381.5 [M+1] (73.5%), 157.2 [M−2(-C_8H_{17})] (97.6%).

1,3,8-Trioctyl-1,8-dihydropyrrolo[3,2-g]indole (**TOBDP**): pinkish yellow oil (1.35 g, 26%); ^{1}H NMR (400 MHz, $CDCl_3$): 7.33−7.35 (d, J = 8.4 Hz, 1H), 7.30−7.32 (d, J = 8.4 Hz, 1H) 6.98−6.99 (d, J = 3.2 Hz, 1H), 6.77 (s, 1H), 6.59−6.60 (d, J = 3.2 Hz, 1H), 4.30−4.34 (t, J = 7.6 Hz, 2H), 4.24−4.28 (t, J = 7.6 Hz, 2H), 2.74−2.78 (t, J = 7.6 Hz, 2H), 1.70−1.88 (m, 6H), 1.24−1.45 (m, 30H), 0.86−0.89 (m, 9H). ^{13}C NMR (100 MHz, $CDCl_3$): 127.5, 126.8, 126.3, 125.0, 124.7, 124.5, 117.8, 113.5, 112.2, 103.5, 50.8, 50.7, 31.9, 31.7, 31.6, 31.2, 31.2, 30.1, 29.7, 29.6, 29.4, 29.2, 29.2, 29.1, 26.8, 25.3, 22.7, 22.6, 14.1, 14.1. APCI-Mass 493.7 [M+1] (100.0%), 381.5 [M− (-C_8H_{17})] (12.0%), 157.1 [M−3(-C_8H_{17})] (32.0%).

Synthesis of tetracyclic fused aromatic pyrrole-based monomers

The tetracyclic fused aromatic pyrrole-based monomer, 1,10-dihydrobenzo[*e*]pyrrolo[3,2-*g*]indole (**NBP**), was synthesized using literature procedure reported by Roznyatovskiy *et al.*[38] Compound **6** was synthesized according to the modified literature procedure reported by Franzen *et al.*[39] Compound **7** and **8** were prepared according to the modified literature procedure reported by

Roznyatovskiy *et al*.[38] 1,10-dihydrobenzo[*e*]pyrrolo[3,2-*g*]indole (**NBP**) was synthesized using modification of the procedure reported by Roznyatovskiy *et al*.[38]

Synthesis of 2,3-dihydrazinylnaphthalene, **6**: The compound **6** was synthesized using a modified literature procedure reported by Franzen *et al*.[40] A two necked round bottom flask was charged with 2,3-dihyroxynaphthalene (6.00 g, 37.50 mmol), 6 mL of hydrazine hydrate (99%) (6.18 g, 123.60 mmol), hydrazine sulphate (2.00 g, 15.38 mmol) and ethanol (2 mL). The solution was refluxed until reaction mixture turned into clear, red liquid. This clear liquid was refluxed for 4 h till slight precipitation began to appear. The reaction mixture was allowed to cool slowly to the room temperature during which time more solids precipitate out. To it, 40 mL dichloromethane and 10 mL methanol was added and solids were quickly filtered off using vacuum filtration, washed with 2 X 10 mL (8:2) dichloromethane-methanol and dried under vacuum to yield air sensitive off white product **6** in 60% yield (4.21 g, 22.35 mmol). As being very unstable, crude product was directly taken for the synthesis of diethyl 2,2′-(naphthalene-2,3-diylbis(hydrazin-2-yl-1-ylidene))(2*E*,2′*E*)-dipropionate, **7** without any characterization.

Synthesis of 2,2′-(naphthalene-2,3-diylbis(hydrazin-2-yl-1-ylidene))(2*E*,2′*E*)-dipropionate, **7**: The compound **7** was synthesized using a modified literature procedure reported by Roznyatovskiy *et al*.[38] To a 250 mL two-necked round bottom flask were added compound **6** (4.21 g, 22.35 mmol) and 56 mL of ethanol. A solution of ethyl pyruvate (6.50 g, 56 mmol) in 5.6 mL of ethanol was added drop wise to this solution. During the addition, slight exothermicity was observed and yellow solids began to precipitate out. After complete addition, the reaction mixture was stirred at room temperature overnight. The light yellow reaction mixture slurry was filtered off and solids were washed with small amount of ethanol and dried under vacuum to yield light yellow product **7** as a mixture of two isomers (symmetrical and non-symmetrical) in 72% yield (6.20 g, 16.15 mmol). This crude mixture was characterized by mass spectroscopy.

2,2′-(Naphthalene-2,3-diylbis(hydrazin-2-yl-1-ylidene))(2E,2′E)-dipropionate, **7**: Light yellow solid (6.20 g, 72%); ESI-Mass 384.17 [M+] (58%). Rest of characterization data were reported by Roznyatovskiy *et al*.[38]

Synthesis of diethyl 1,10-dihydrobenzo[*e*]pyrrolo[3,2-*g*]indole-2,9-dicarboxylate, **8**: Compound **8** was synthesized using literature procedure reported by Roznyatovskiy *et al*.[38] Compound **7** (3.00 g, 7.81 mmol), tosic acid mono-hydrate (14.84 g, 78.12 mmol) and ethanol (0.1 M, 78 mL) were charged in a two necked round bottom flask and heated to reflux for 3 h. After completion of reaction as indicated by TLC, reaction mixture was allowed to cool at room temperature during which the product precipitated out. The product was filtered off using vacuum filtration, washed with small amount of ethanol, and dried under vacuum.

Diethyl 1,10-dihydrobenzo[*e*]pyrrolo[3,2-*g*]indole-2,9-dicarboxylate, **8**: Bluish white solid (2.20 g, 80%); ^{1}H NMR (400 MHz, DMSO-D_6): 11.89 (s, 1H), 8.32−8.34 (dd, J_1 = 6.0 Hz; J_2 = 3.2 Hz, 1H), 7.83−7.84 (d, J = 2.4 Hz, 1H), 7.46−7.48 (dd, J_1 = 6.0 Hz; J_2 = 3.2 Hz, 1H), 4.38−4.42 (q, J = 7.2 Hz, 2H), 1.37-1.40 (t, J = 7.2 Hz, 3H). ESI-Mass 350.16 [M+] (67%), 349.16 [M−1(-H)] (66%). All other characterization data were reported in literature.[38]

Synthesis of 1,10-dihydrobenzo[*e*]pyrrolo[3,2-*g*]indole (**NBP**): The tetracyclic compound **NBP** was synthesized using modification of the literature procedure reported by Roznyatovskiy et al.[38] Compound **8** (2.50 g, 7.14 mmol), ethylene glycol (40 mL), and KOH (4.0 g, 71.4 mmol) was taken in a round bottom flask, kept under high vacuum for 1 h. The mixture was then heated at reflux for 3 h under nitrogen atmosphere. After completion of reaction, the reaction mixture was cooled to 70 °C and degassed water (90 mL) added to it and stirred for 5 min. It is further cooled to room temperature and the off white to yellow colored precipitates thus formed were filtered by vacuum filtration, washed thoroughly with water to remove the excess ethylene glycol, dried and finally washed with hexanes to obtain off white solids. The pure product **NBP** was obtained by subjecting the crude product to the flash column chromatography over silica gel and using dichloromethane as eluent.

1,10-Dihydrobenzo[*e*]pyrrolo[3,2-*g*]indole (**NBP**): Off white solid (0.95 g, 64%); ^{1}H NMR (400 MHz, DMSO-D_6): 10.99 (s, 2H), 8.17−8.20 (dd, J_1 = 6.4 Hz; J_2 = 3.6 Hz, 1H), 7.35−7.37 (dd, J_1 = 6.4 Hz; J_2 = 3.6 Hz, 1H), 7.25−7.26 (m, 1H), 7.02−7.03 (dd, J_1 = 3.2 Hz; J_2 = 2.4 Hz, 1H). ^{13}C NMR (100 MHz, $CDCl_3$): 124.9, 123.9, 123.5, 121.3, 120.5, 119.8, 102.7. ESI-Mass 206.2 [M+] (100%), 204.8 [M−1(-H)] (94%).

Synthesis of 1,10-dioctyl-1,10-dihydrobenzo[*e*]pyrrolo[3,2-*g*]indole (**DONBP**):

The pure compound **NBP** (1.00 g, 4.85 mmol) was dissolved in DMF (100 mL). To this, sodium hydroxide flakes (1.94 g, 48.54 mmol) was added and the resulting suspension was stirred at room temperature for 10 min. To this stirred solution was added, *n*-octylbromide (5.62 g, 29.12 mmol) drop wise over a period of 5 min. After the complete addition, reaction mixture was stirred at 80 ^{o}C for 3 h and monitored by TLC. After completion of the reaction, as indicated by TLC, 400 mL of water was added to it and extracted with aliquots of dichloromethane (2 X 50 mL). Combined organic layers are washed with saturated brine solution, water and dried over anhydrous $MgSO_4$. Crude product is obtained after evaporation of solvent which is subjected to the column chromatography over silica gel using 1% ethyl acetate-petroleum ether as an eluent.

1,10-Dioctyl-1,10-dihydrobenzo[*e*]pyrrolo[3,2-*g*]indole (**DONBP**): Light yellow oil (1.56 g, 75%); ^{1}H NMR (400 MHz, $CDCl_3$): 8.20−8.24 (dd, J_1 = 6.4 Hz; J_2 = 3.6 Hz, 1H), 7.44−7.48 (dd, J_1 = 6.4 Hz; J_2 = 3.6 Hz, 1H), 7.12−7.13 (d, J = 3.2 Hz, 1H), 7.05−7.06 (d, J = 2.8 Hz, 1H), 4.36−4.40 (t, J = 7.6 Hz, 2H), 1.84−1.89 (m, 2H), 1.22−1.28 (m, 10H), 0.85−0.89 (t, J = 7.2 Hz, 3H). ^{13}C NMR (100 MHz, CDCl3): 121.9, 120.4, 118.9, 118.7, 118.4, 118.0, 97.7, 46.3, 26.9, 26.4, 24.4, 24.3, 21.9, 17.8, 9.3. APCI-Mass 431.5 [M+1] (100%), 432.5 [M+2] (39%).

Spectral data

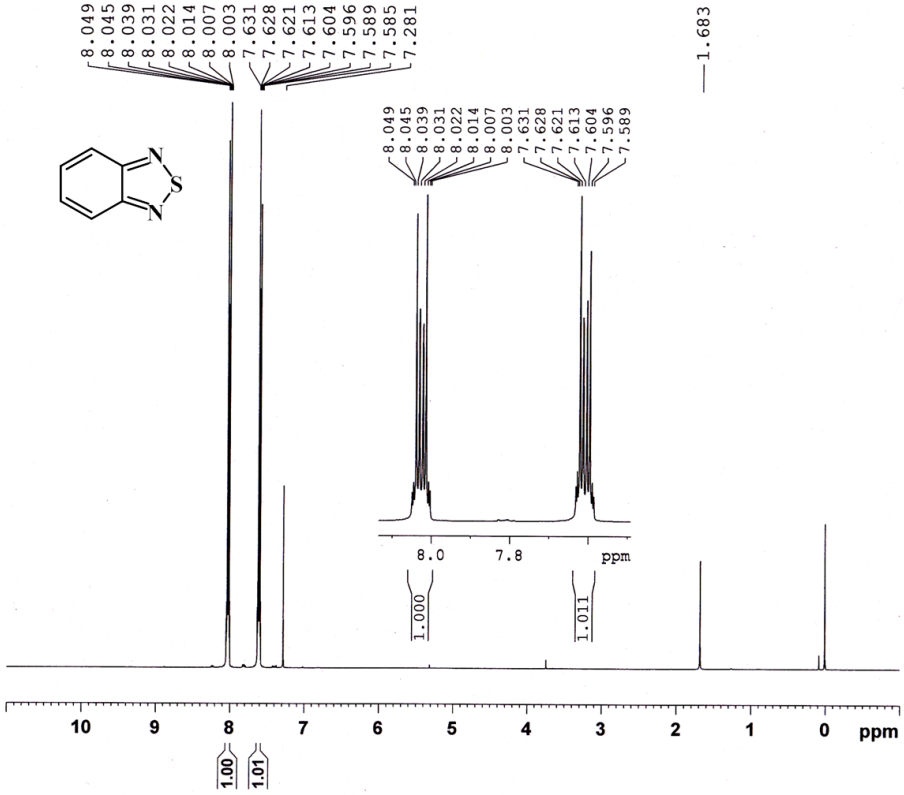

Figure 2.11 ^{1}H NMR spectrum of compound **1**

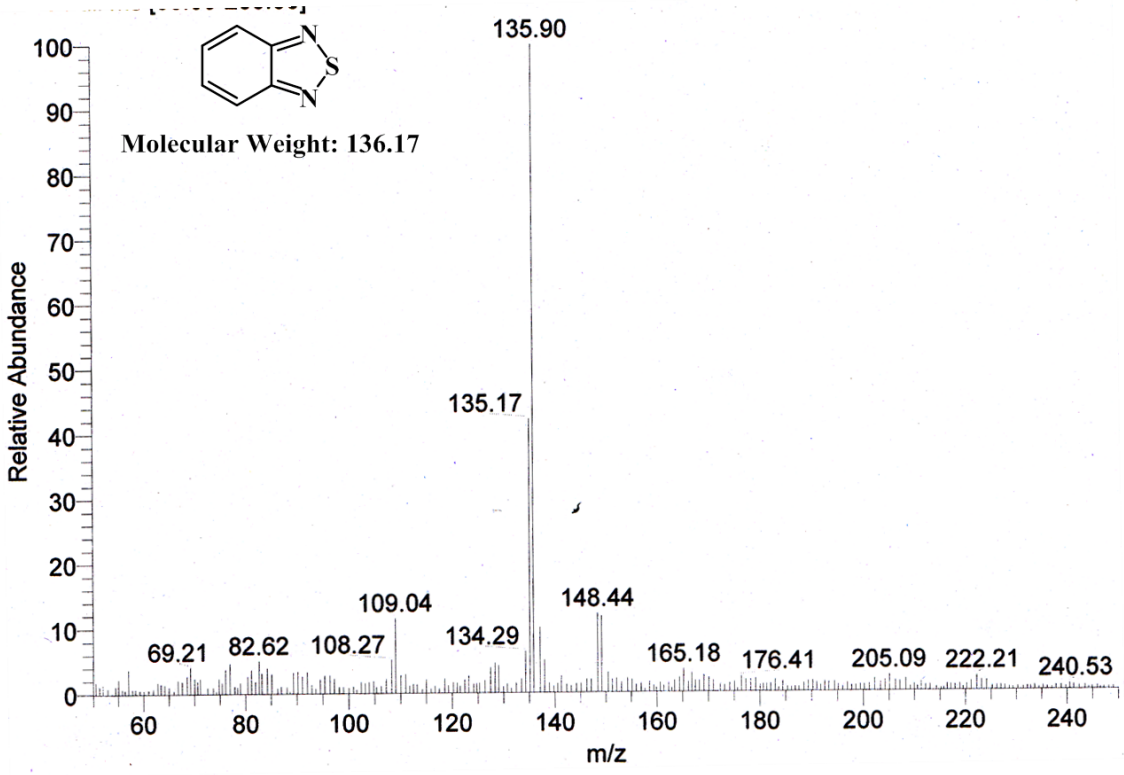

Figure 2.12 ESI-Mass spectrum of compound **1**

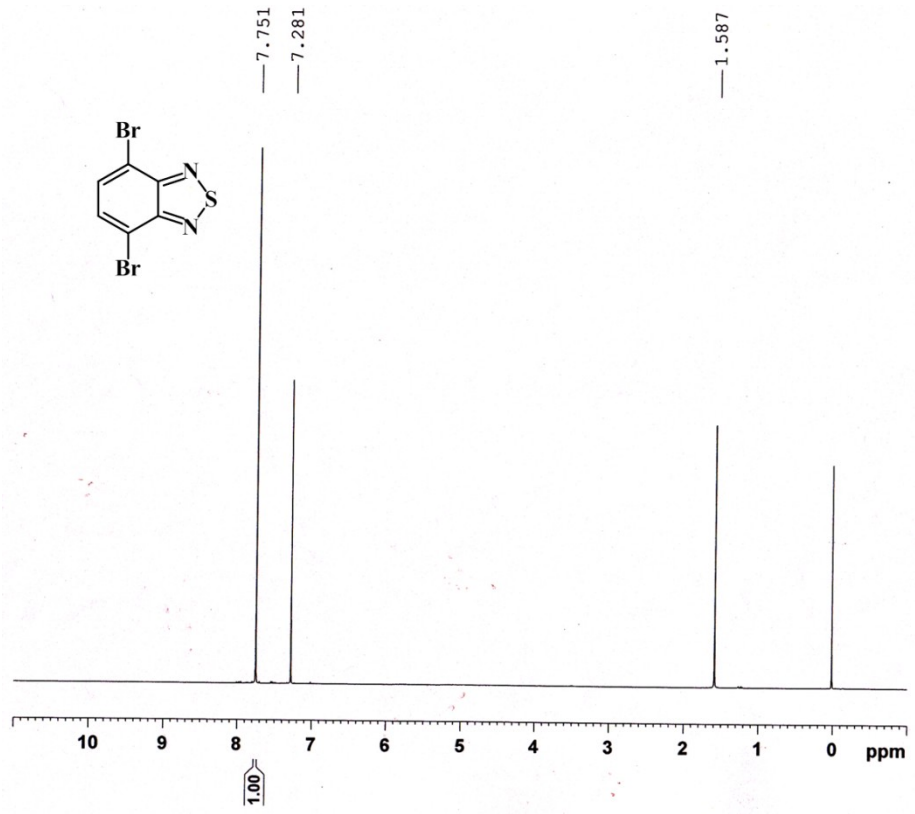

Figure 2.13 ^{1}H NMR spectrum of compound **2**

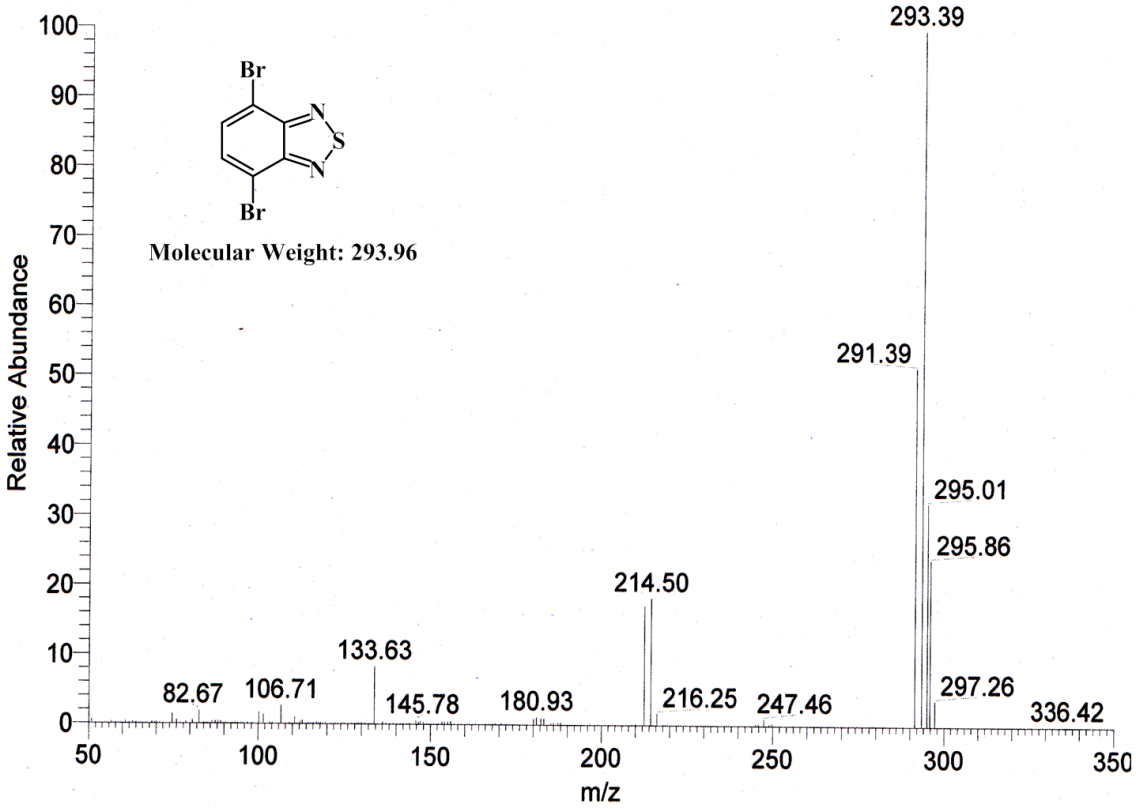

Figure 2.14 ESI-Mass spectrum of compound **2**

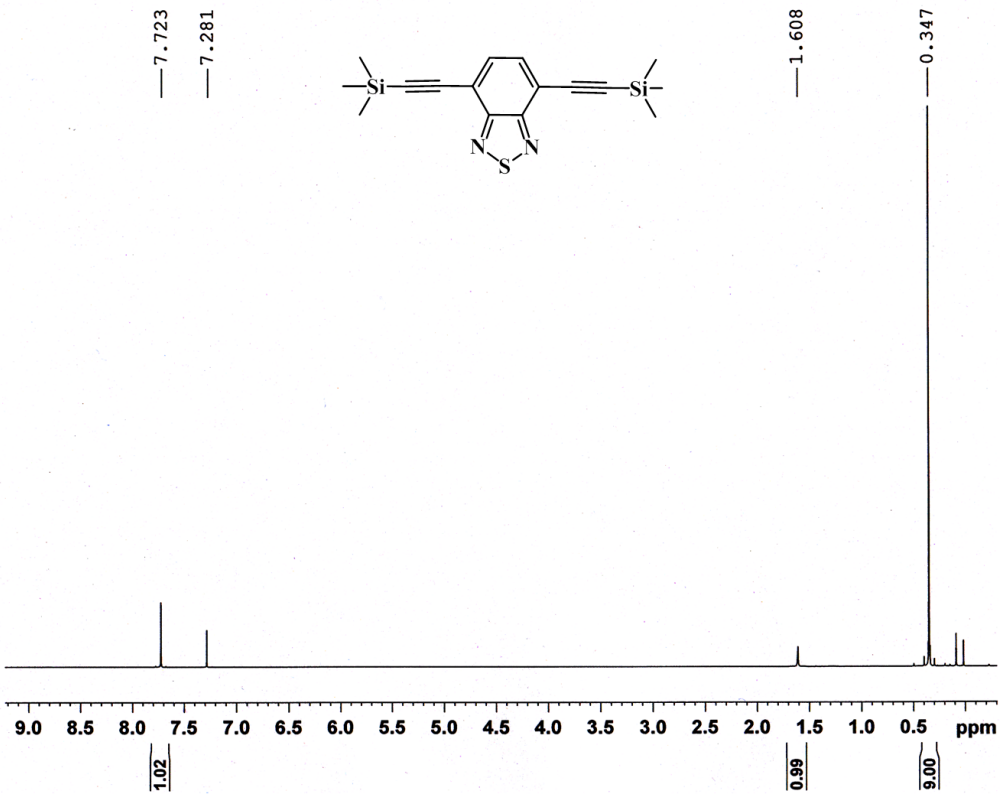

Figure 2.15 ^{1}H NMR spectrum of compound **3**

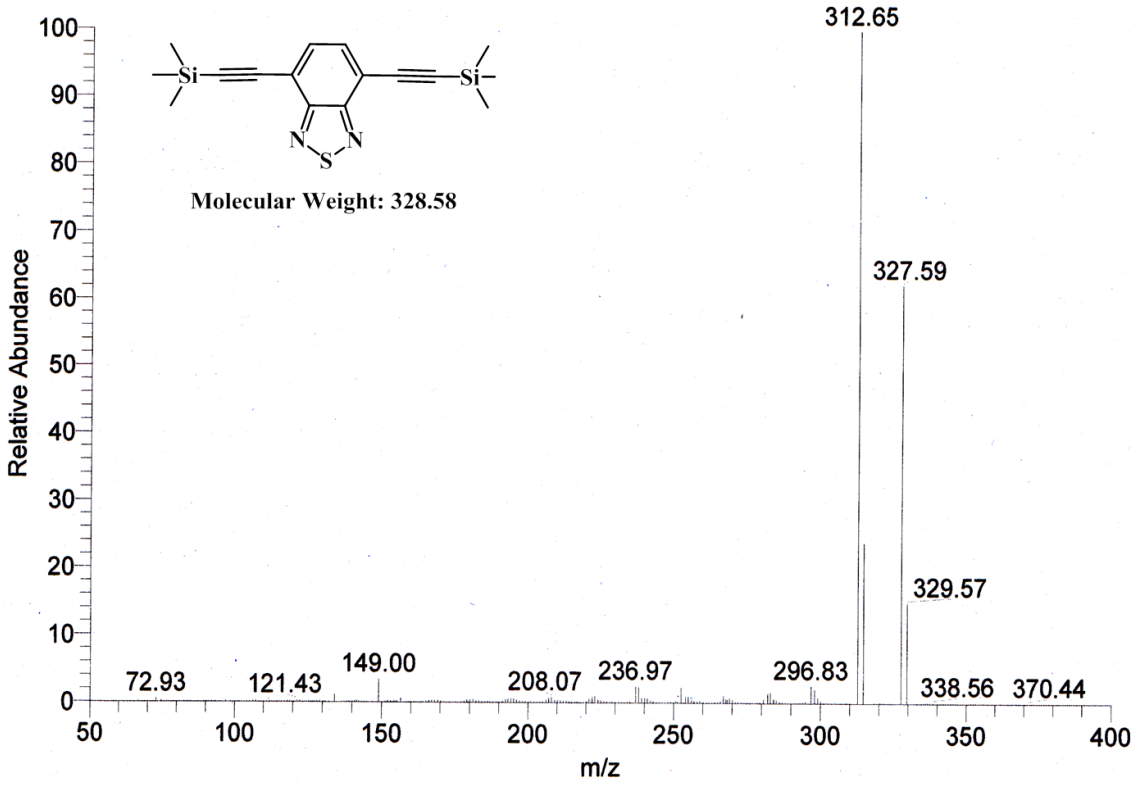

Figure 2.16 ESI-Mass spectrum of compound **3**

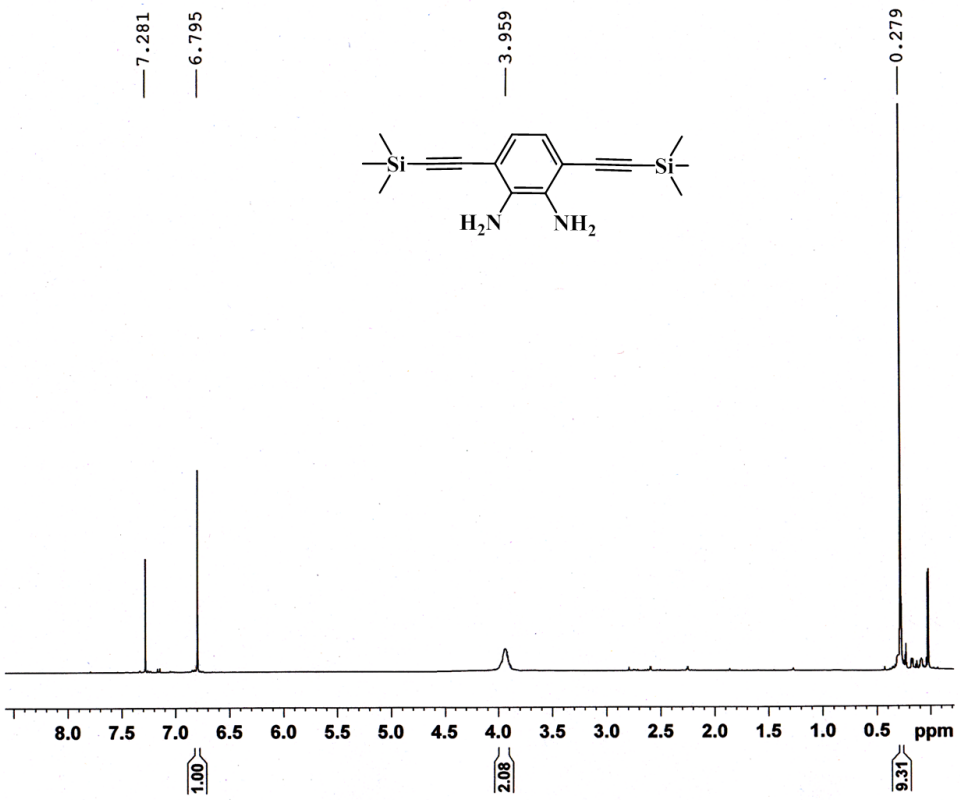

Figure 2.17 ^{1}H NMR spectrum of compound **4**

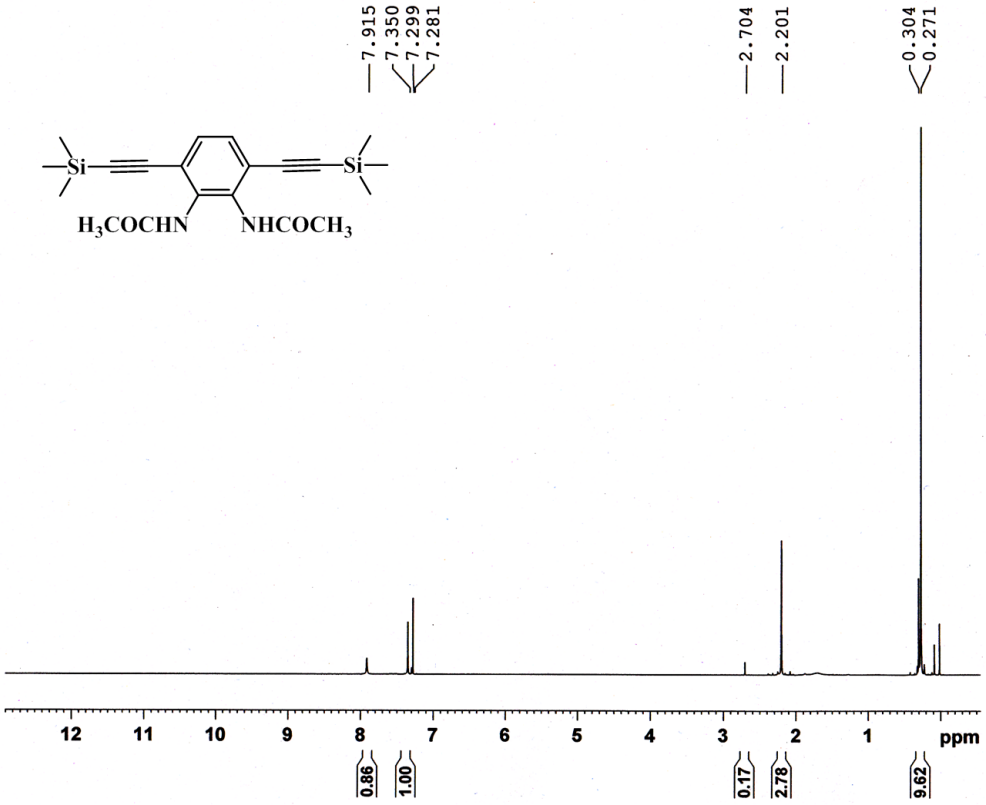

Figure 2.18 ^{1}H NMR spectrum of compound **5**

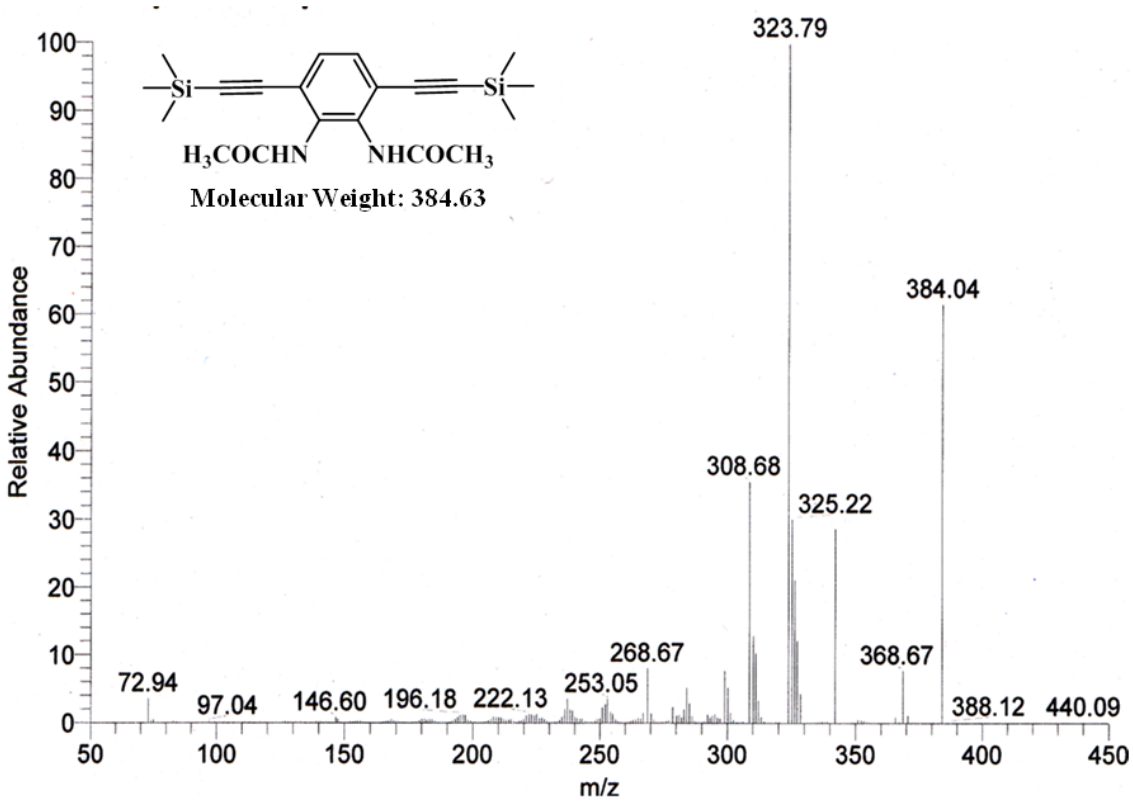

Figure 2.19 ESI-Mass spectrum of compound **5**

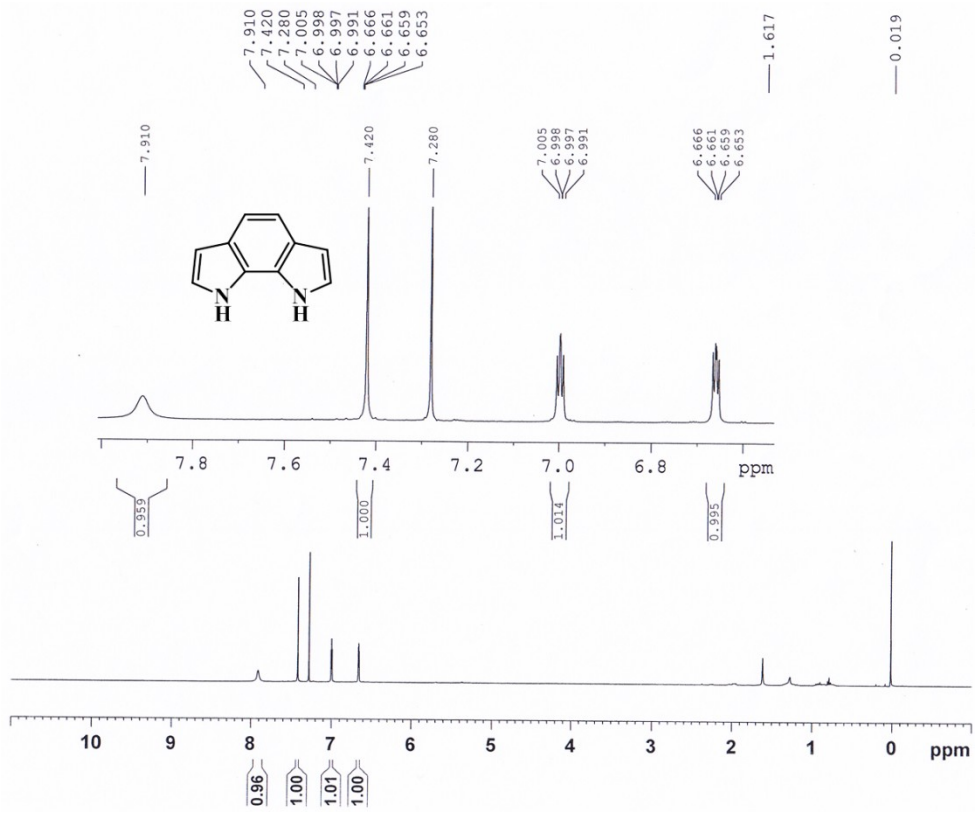

Figure 2.20 ^{1}H NMR spectrum of **BDP**

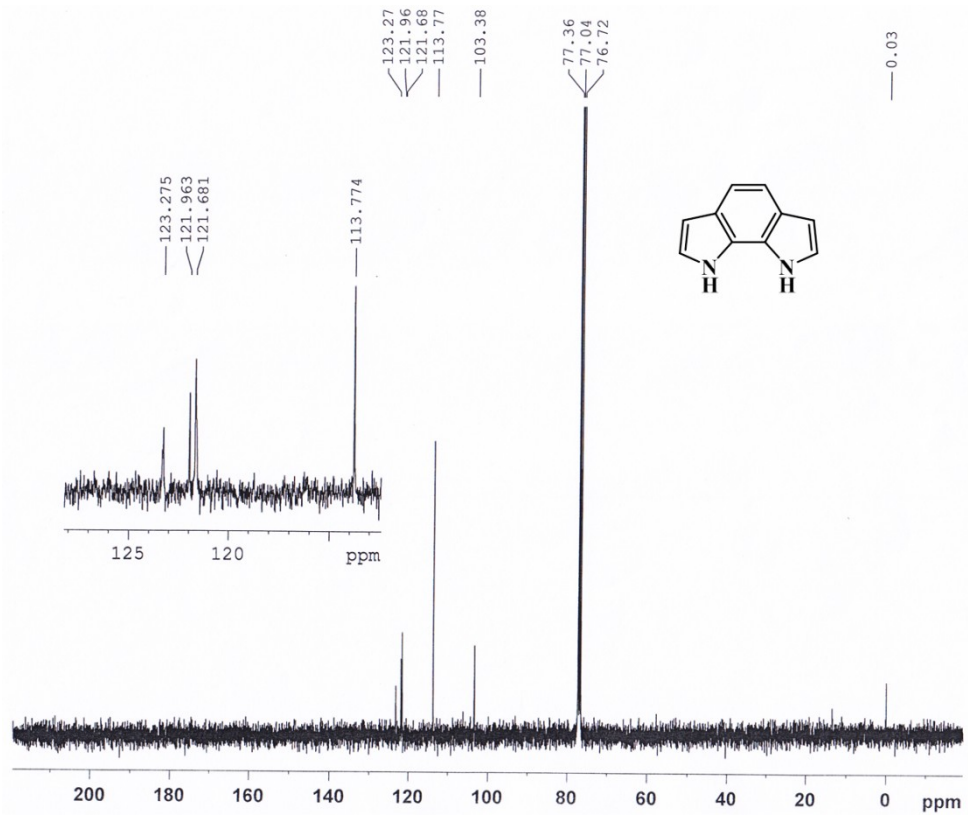

Figure 2.21 ^{13}C NMR spectrum of **BDP**

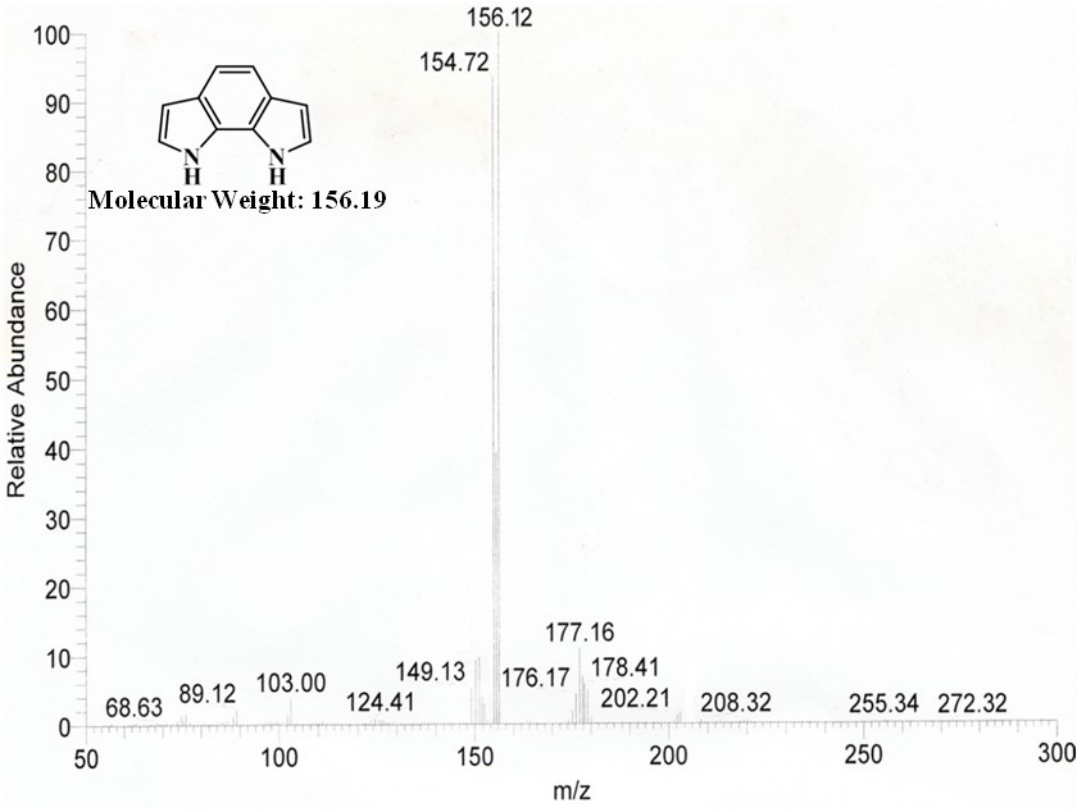

Figure 2.22 ESI-Mass spectrum of **BDP**

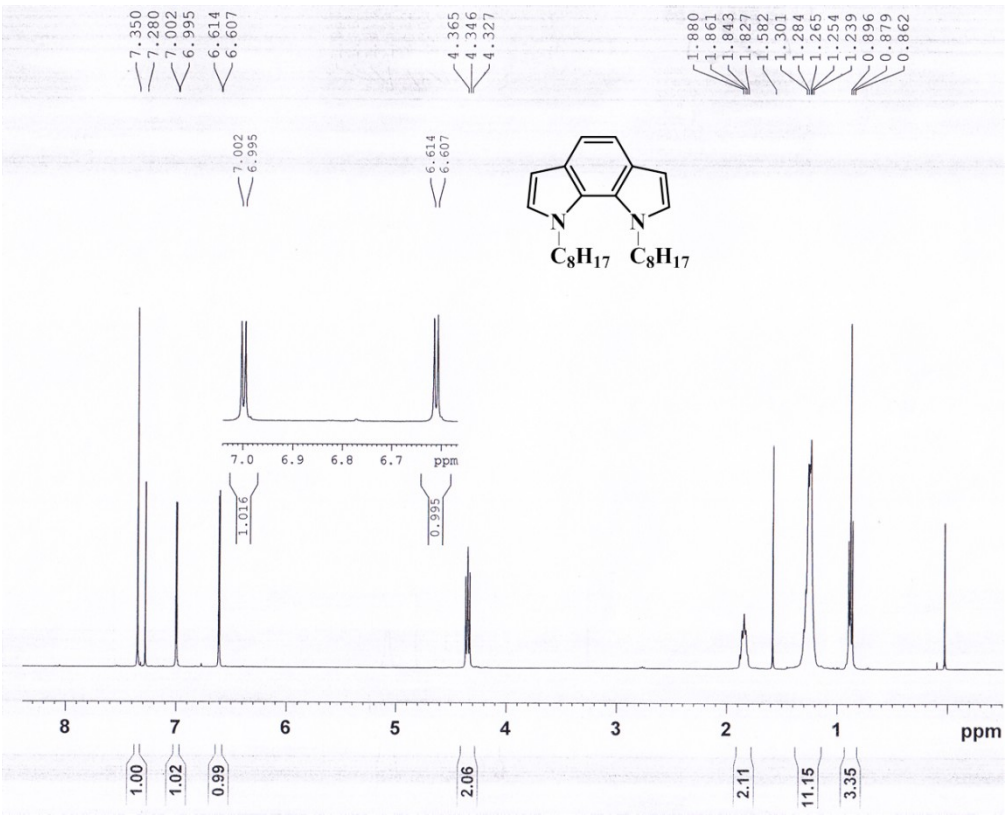

Figure 2.23 ^{1}H NMR spectrum of **DOBDP**

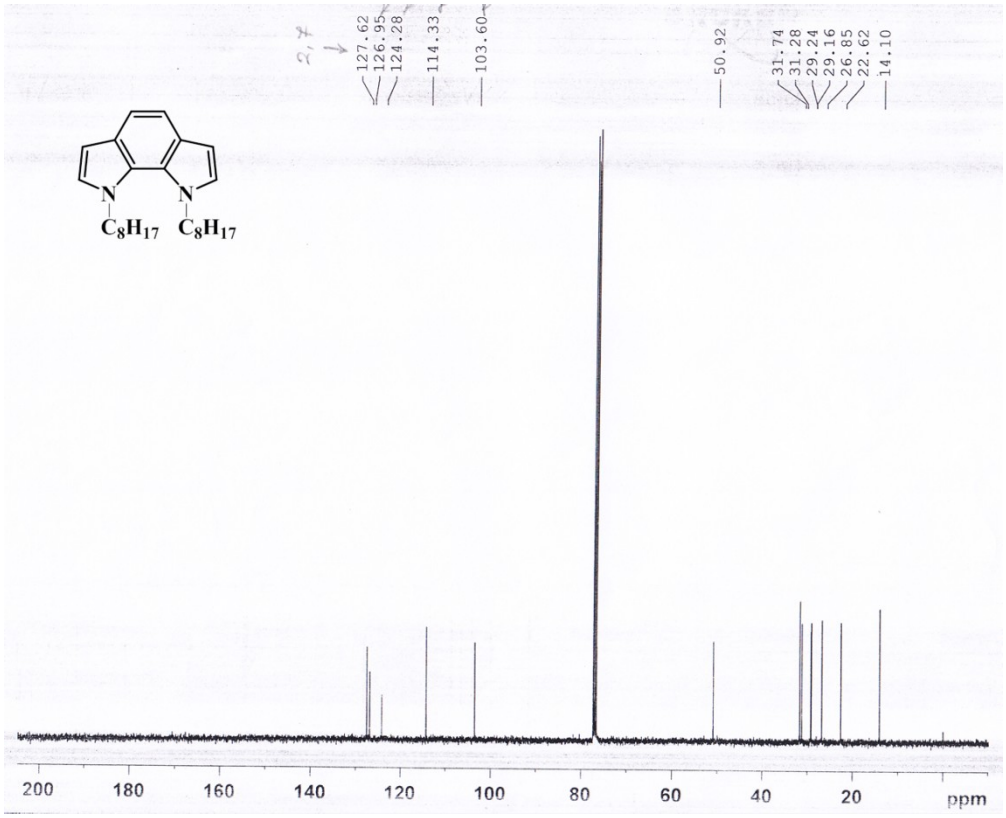

Figure 2.24 ^{13}C NMR spectrum of **DOBDP**

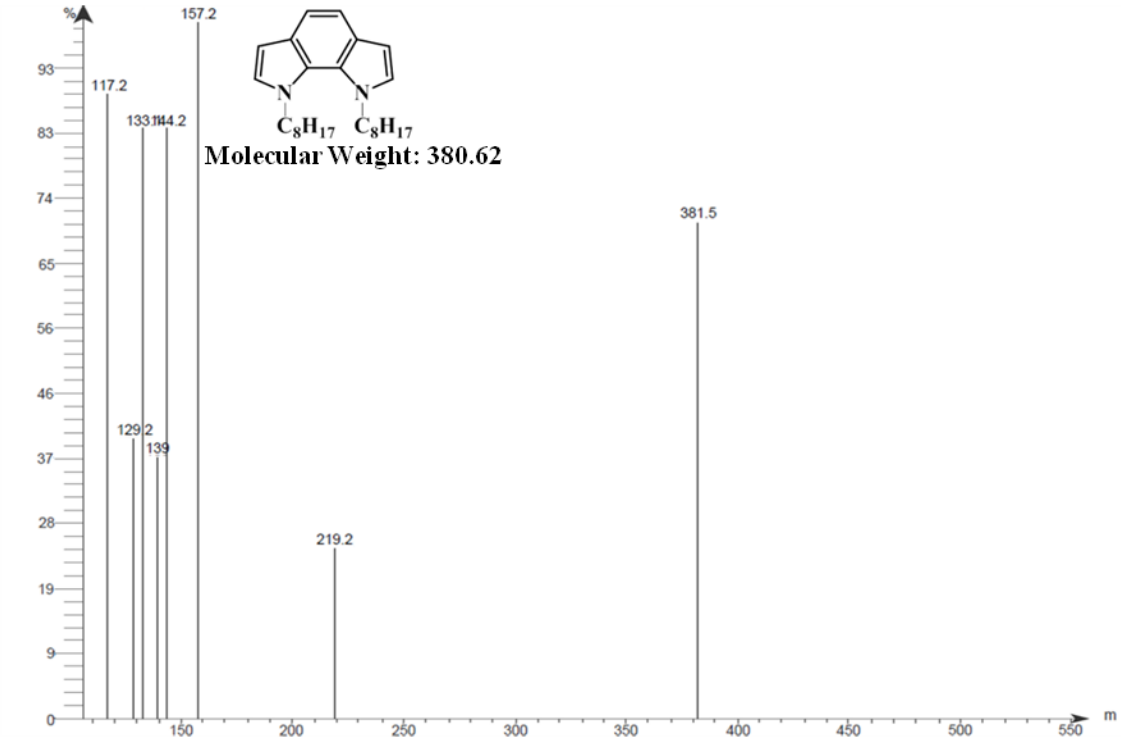

Figure 2.25 APCI-Mass spectrum of **DOBDP**

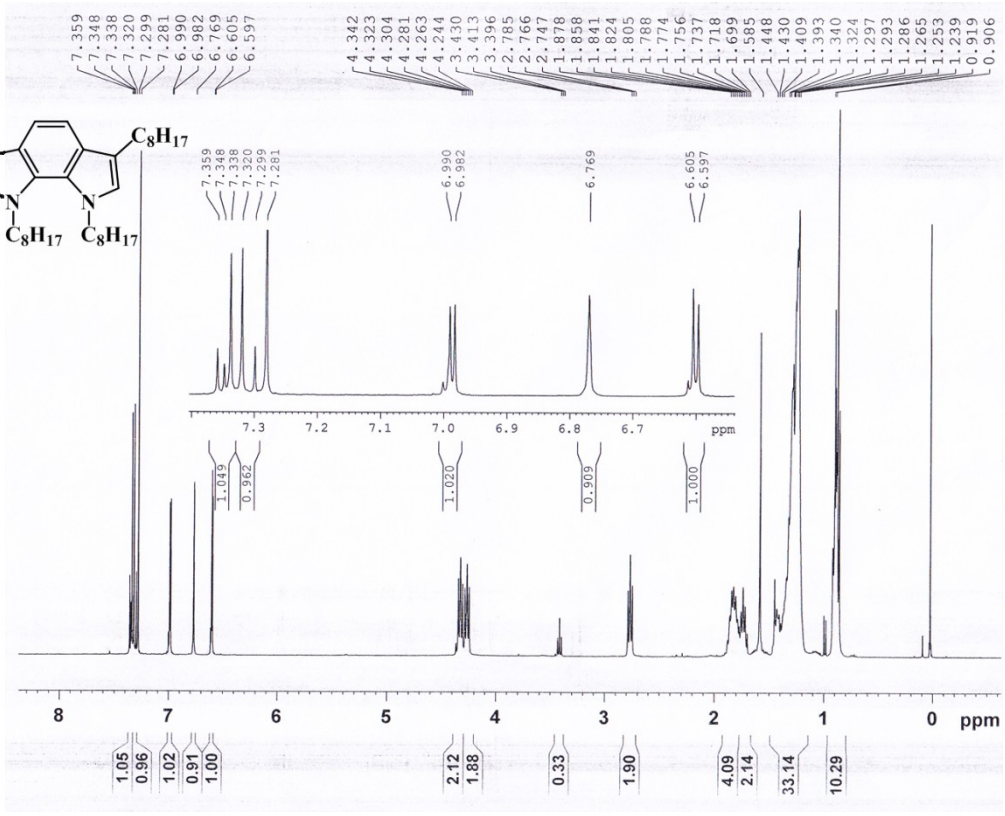

Figure 2.26 ^{1}H NMR spectrum of **TOBDP**

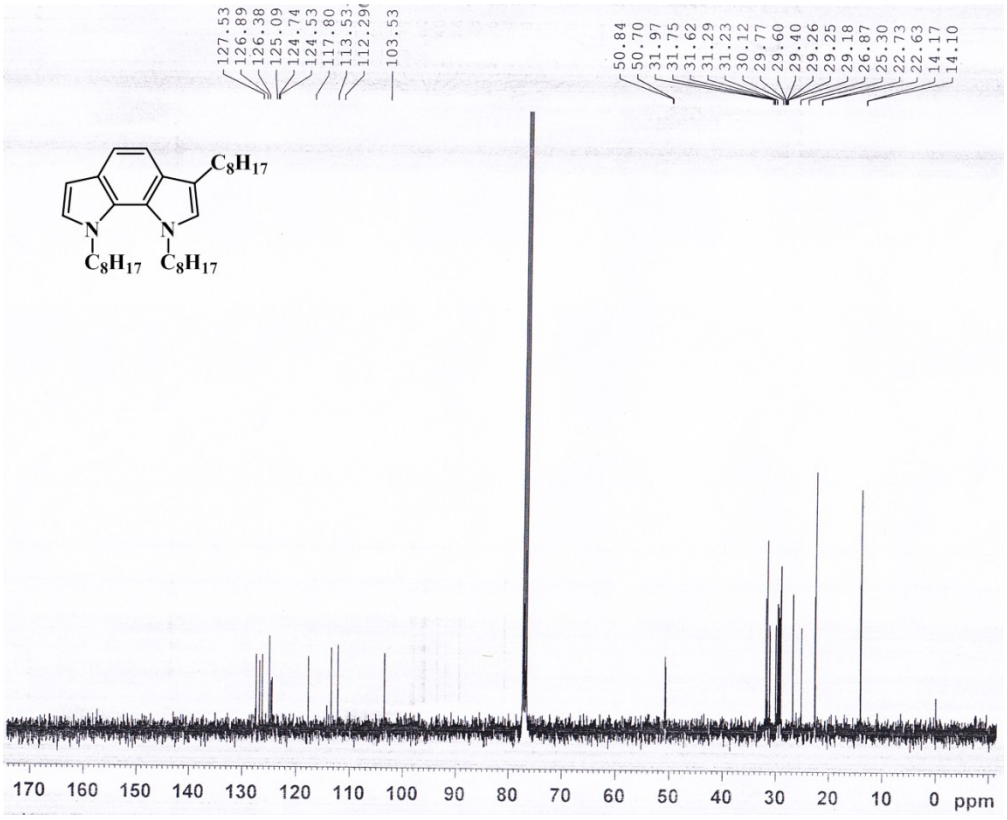

Figure 2.27 ^{13}C NMR spectrum of **TOBDP**

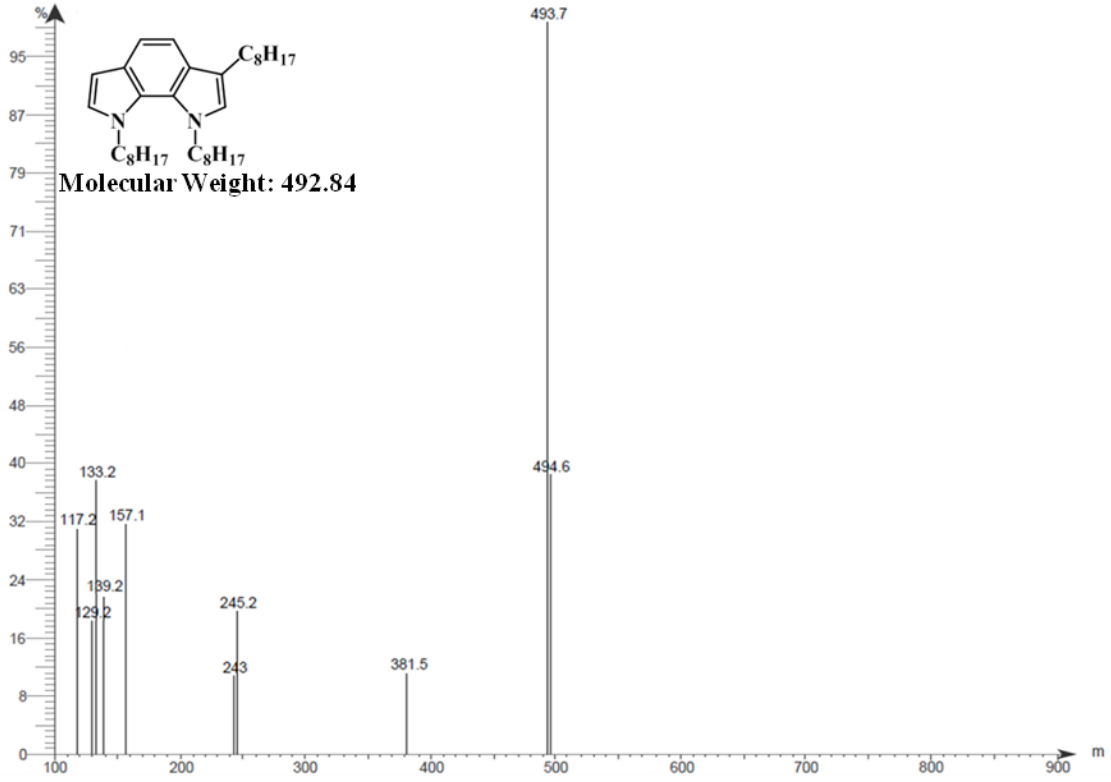

Figure 2.28 APCI-Mass spectrum of **TOBDP**

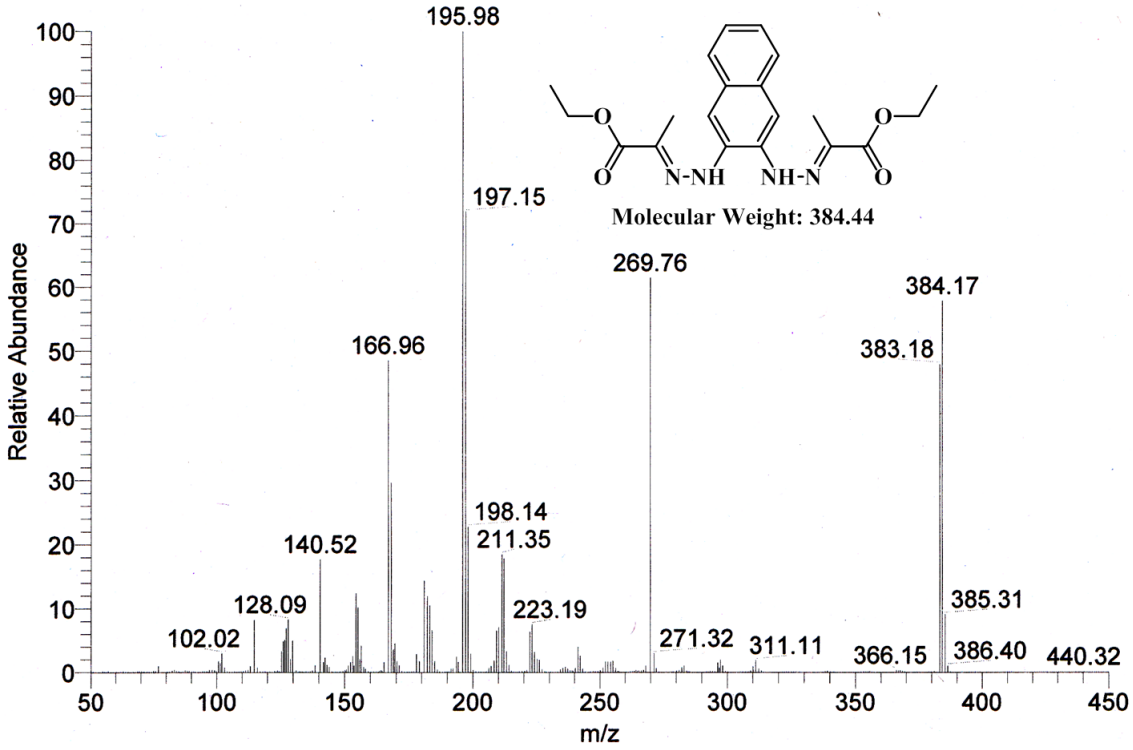

Figure 2.29 ESI-Mass spectrum of compound **7**

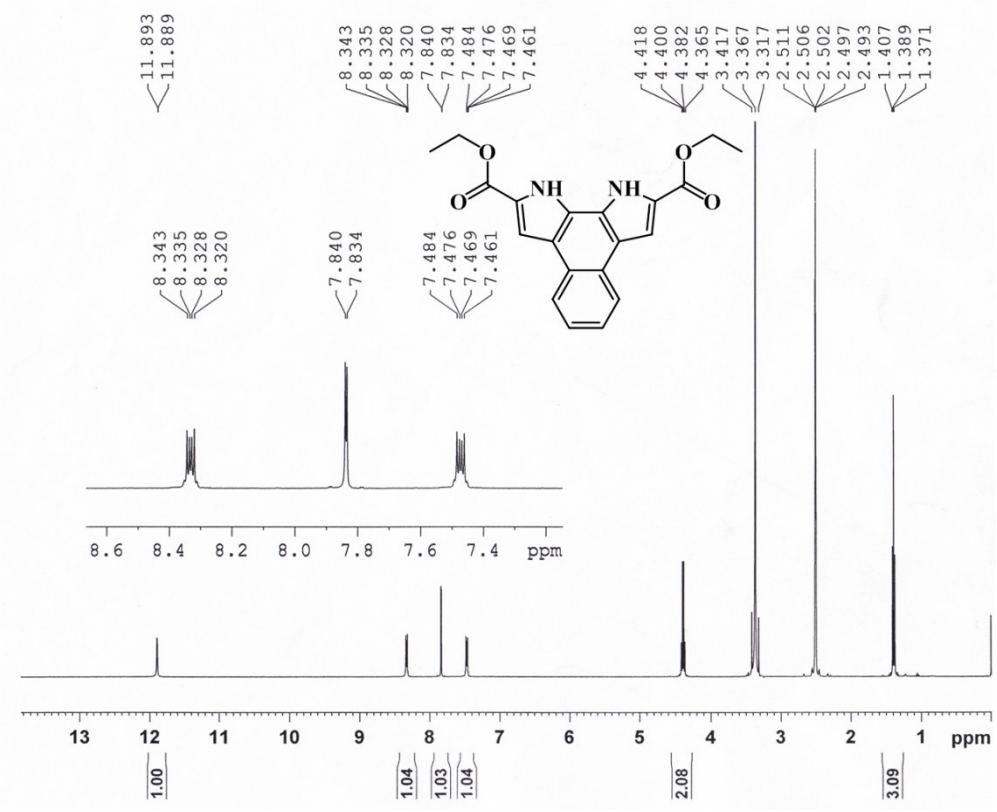

Figure 2.30 ^{1}H NMR spectrum of compound **8**

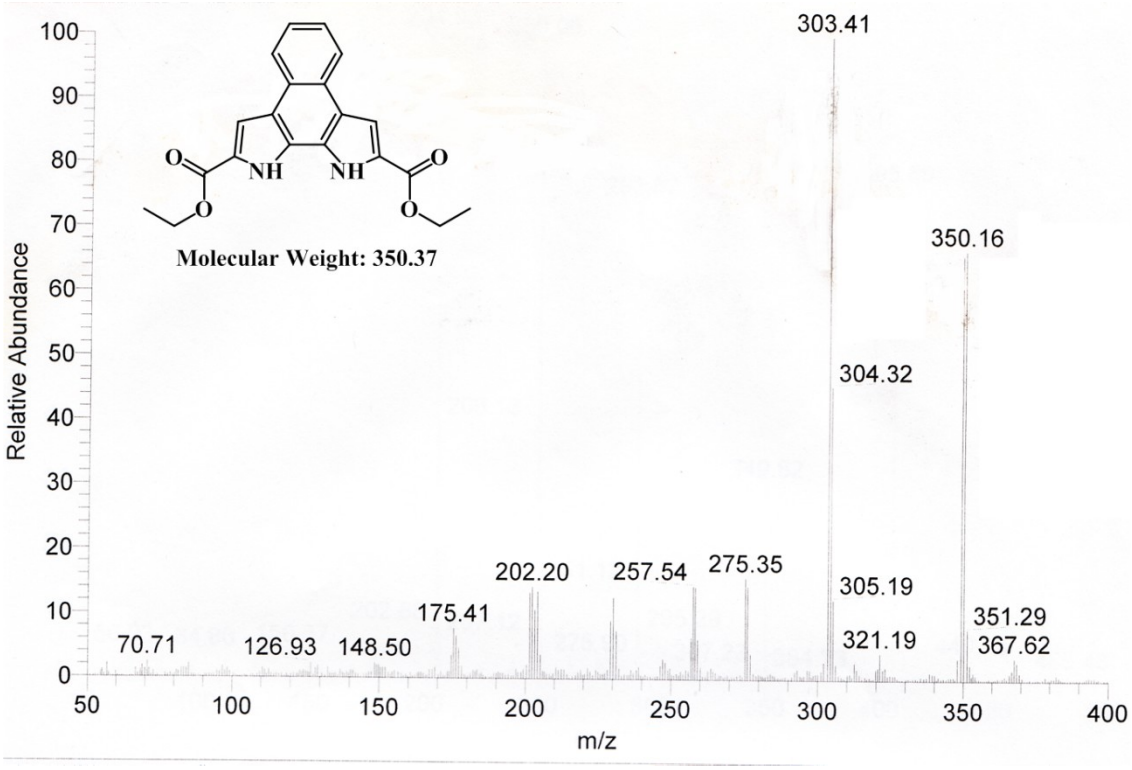

Figure 2.31 ESI-Mass spectrum of compound **8**

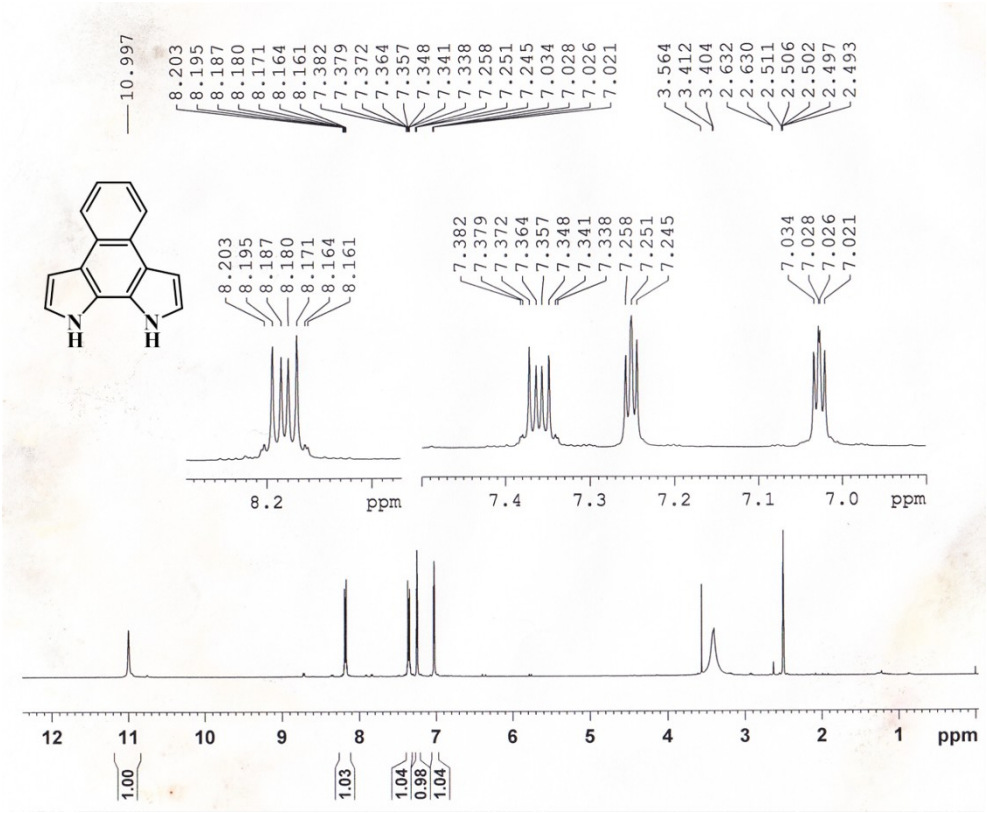

Figure 2.32 ^{1}H NMR spectrum of **NBP**

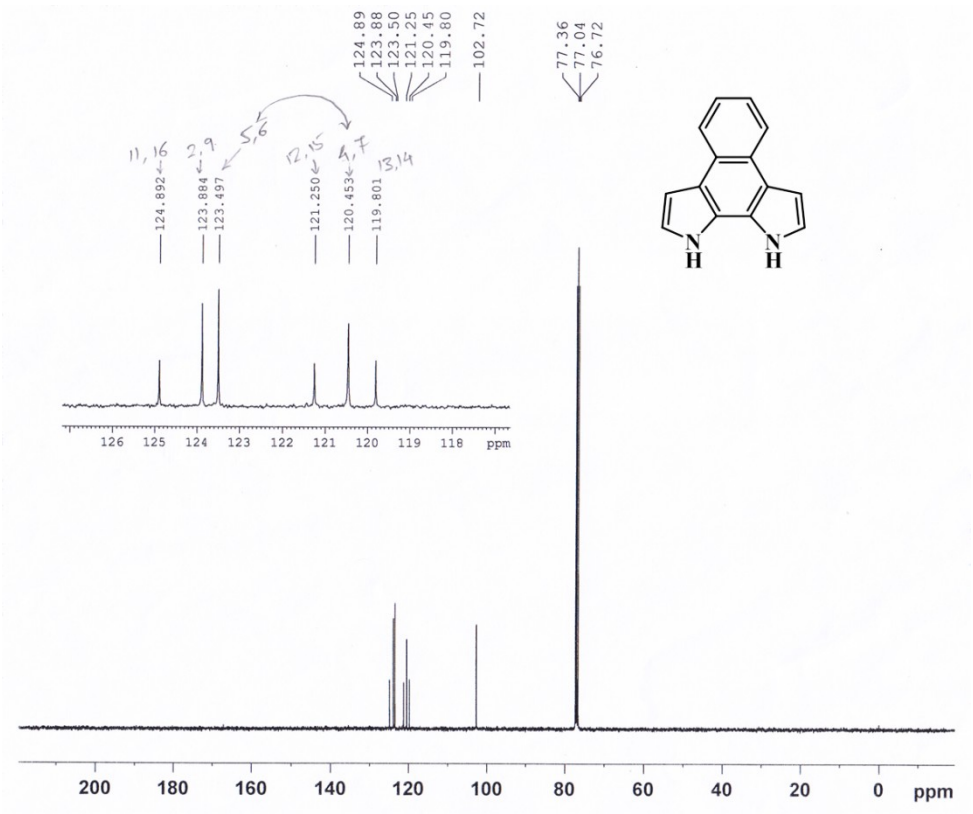

Figure 2.33 ^{13}C NMR spectrum of **NBP**

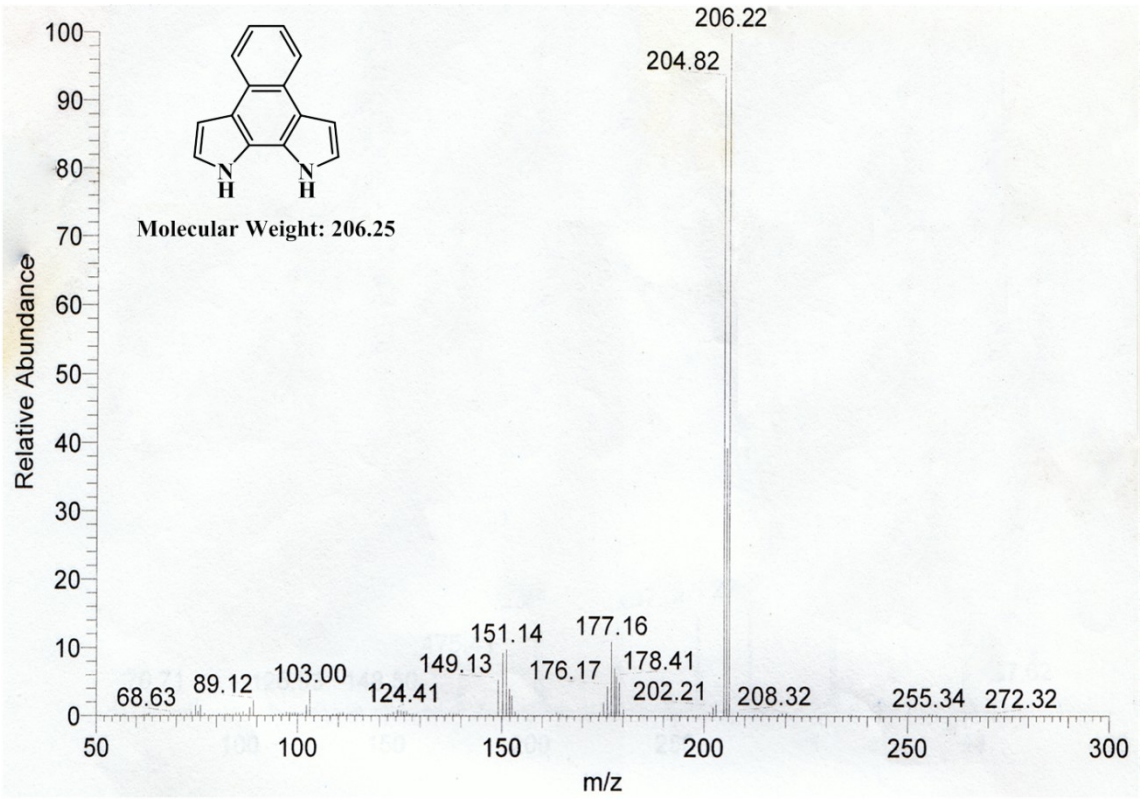

Figure 2.34 ESI-Mass spectrum of **NBP**

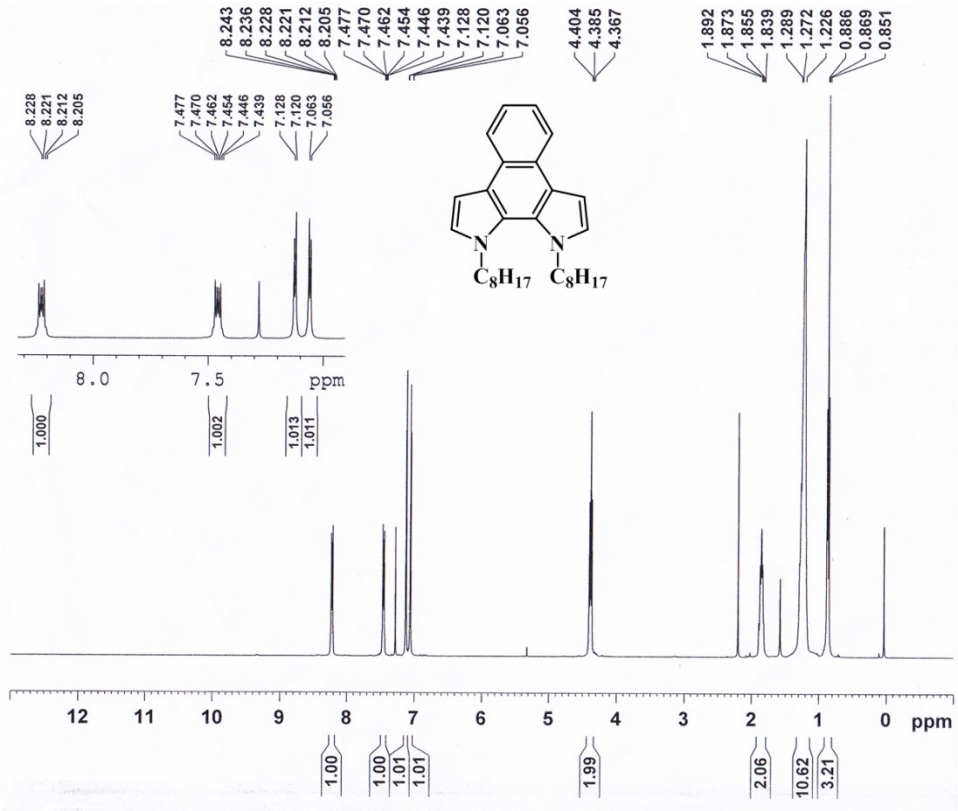

Figure 2.35 ^{1}H NMR spectrum of **DONBP**

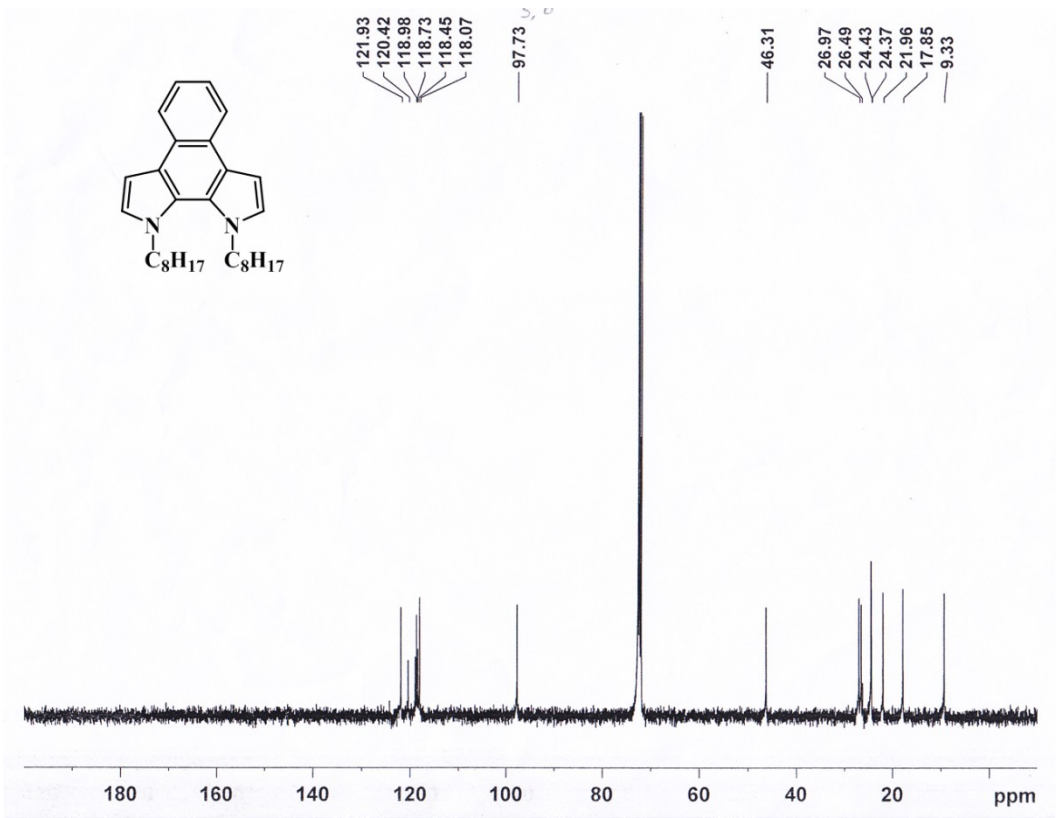

Figure 2.36 ^{13}C NMR spectrum of **DONBP**

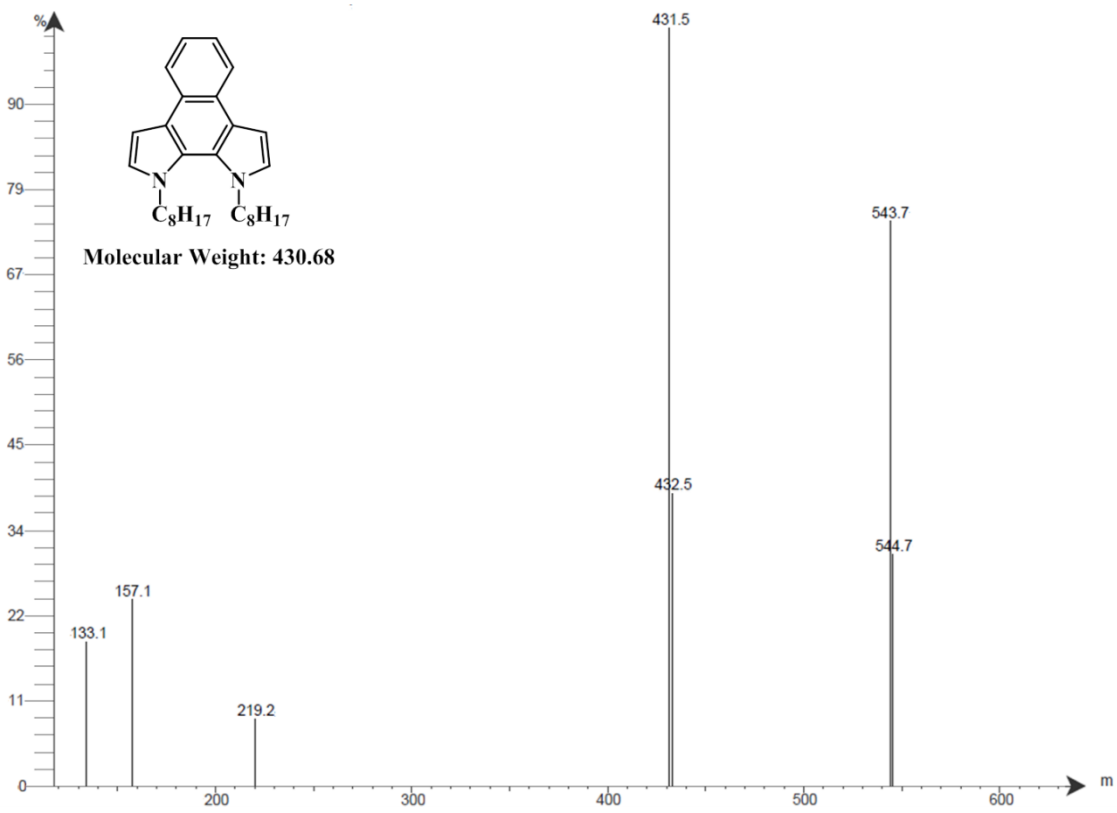

Figure 2.37 APCI-Mass spectrum of **DONBP**

Part-B: Synthesis, characterization and electrochemistry of conjugated polymers

Results and discussion

Electrochemical polymerization of synthesized monomers

Electrochemical polymerization technique has advantage that it forms a layer of conducting material directly onto the surface of electrode, so that solubility and processability needs for the synthesized polymers can be avoided. Five membered heterocyclic molecule pyrrole and pyrrole-based molecules are well-known for its reactivity towards oxidative polymerization. The synthesized monomers **DOBDP**, **NBP** and **DONBP** were electrochemically polymerized using a three electrode cell comprising Pt-disc working electrode, Pt-wire counter electrode and non-aqueous Ag/Ag^{+} reference electrode. The monomers were dissolved in dry acetonitrile (~5 mM) along with $TBAPF_6$ as a supporting electrolyte and were scanned for repeated CV cycles to see the electrochemical polymerization ability of the monomers at applied anodic potentials. Electrochemical polymerization of monomers **BDP**, **DOBDP**, **NBP** and **DONBP** were attempted under similar electrochemical conditions and were scanned for repeated CV cycles.

Monomer **BDP** oxidized by the applied voltage, but surprisingly did not yielded polymeric film on the working electrode and in CV data, no increase in the current intensity was observed during the subsequent cycling, instead black polymeric particles were observed precipitating out from the electrolytic solution. The possible reason for not getting electro-active polymer layer on the working electrode might be the active involvement of both α- and β- pyrrolic positions in the polymerization, i.e., when **BDP** is oxidized by applying the voltage, polymer formation occurs by the both α-α' and β-β' linkage, resulting into the branched polymer with irregularities rather forming a linear polymer. Also, monomers **DOBDP** and **DONBP** responded to electrochemical polymerization but failed to form continuous films coating at the electrode surface, which can be explained by the stability of the cationic intermediates, i.e., the cationic intermediates which were produced on the electrode surface, were being sufficiently

stable to diffuse away from the electrode rather than being captured by other molecules of the compound to generate polymeric film on the electrode (Figure 2.38 and 2.39).[41]

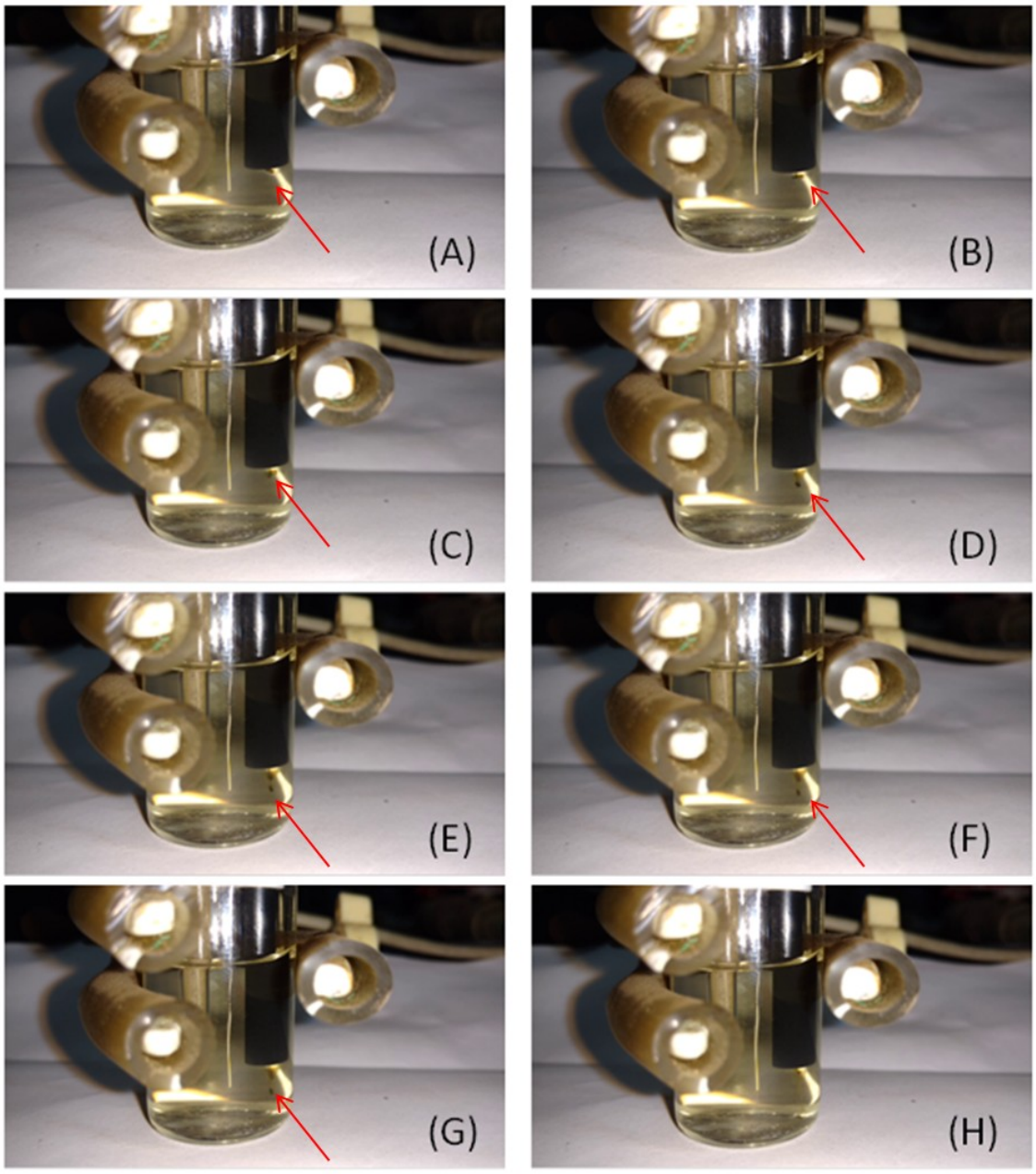

Figure 2.38 Photographs of electro-chemical polymerization of **DOBDP** showing diffusion of the cationic intermediates being formed on the working electrode surface in the electrolytic solution

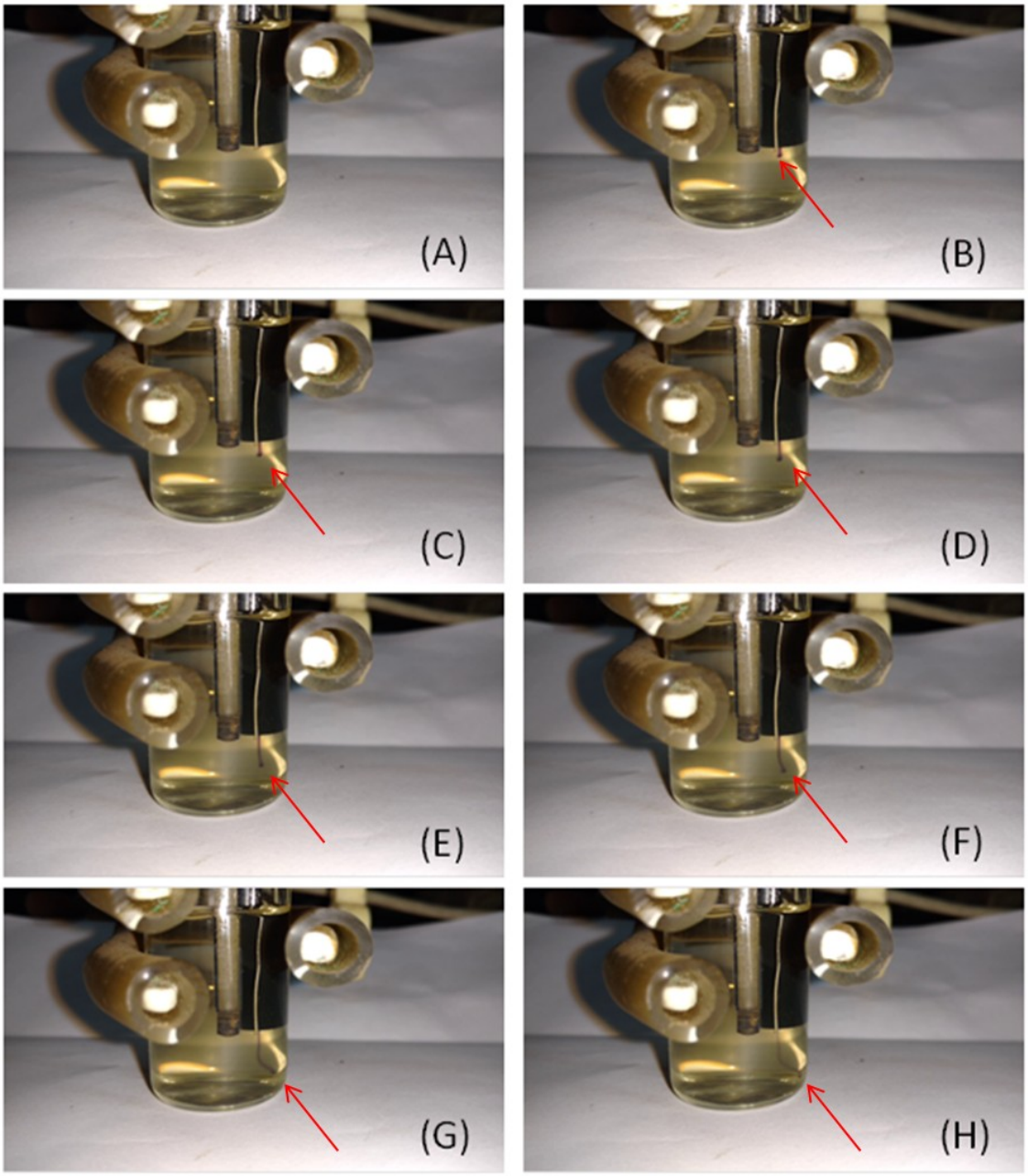

Figure 2.39 Photographs of electro-chemical polymerization of **DONBP** showing diffusion of the cationic intermediates being formed on the working electrode surface in the electrolytic solution

The electrochemical polymerization of **NBP** (Scheme 2.3) afforded continuous polymeric film coating at the electrode surface when cycled repeatedly between −0.2 V to 1.1 V. The CV data of the electro-chemical polymerization of **NBP** (Figure 2.40), showed considerable increase in the current intensity which may be attributed to the deposition of electro-active material on Pt disc electrode. Also, during the subsequent cycles an additional oxidation peak developed at the anodic peak potential +0.47 V which can be ascribed to the oxidation of polymer film formed on the working

electrode. Along with that, an anodic shift was observed in anodic peak potential of the oxidation peak to +0.86 V.

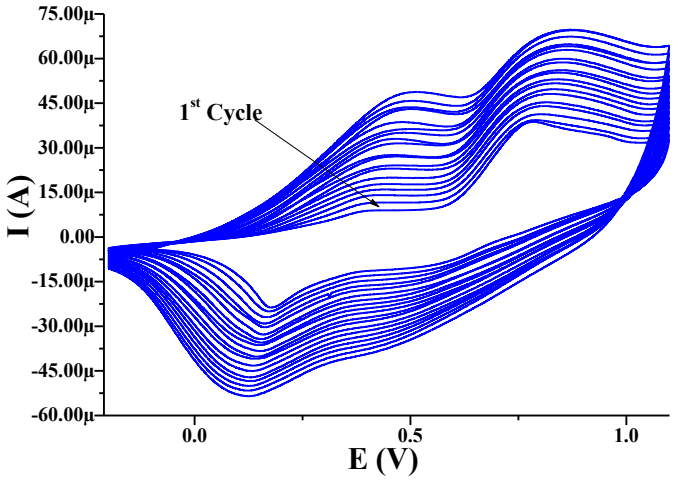

Figure 2.40 Electrochemical polymerization of **NBP** (~5 mM) at 50 mV/s in acetonitrile using $TBAPF_6$ as supporting electrolyte, $E_{onset\ (Fc/Fc+)}$ = 0.36 V

The possible mechanism of the electrochemical polymerization of **NBP** is shown on the Figure 2.41. The process of polymerization involves formation of radical cation by loss of two electrons from the both α- and α′- positions of **NBP** which than undergoes radical-radical bond formation between two monomers and followed by the loss of two protons (Figure 2.41).

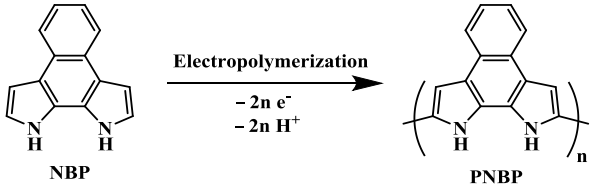

Scheme 2.3 Synthesis of **PNBP** from **NBP** *via* electrochemical polymerization

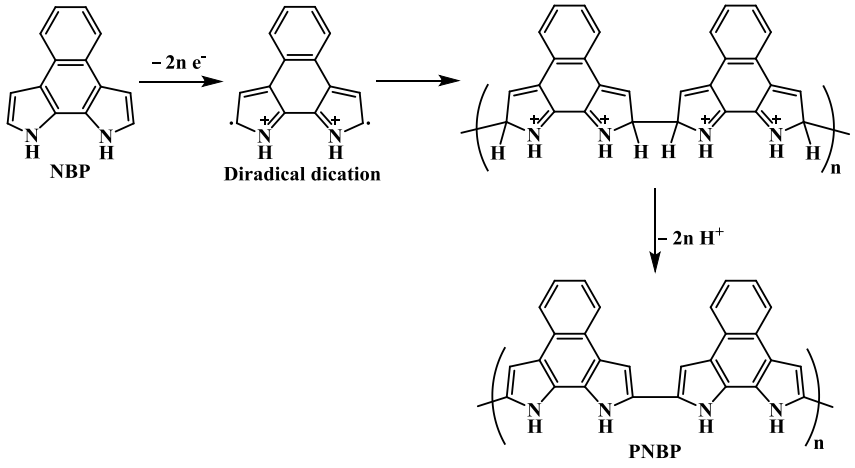

Figure 2.41 Possible mechanism of electrochemical polymerization of **NBP**

Electrochemical properties of PNBP

The frontier orbital energy levels of the synthesized polymer **PNBP** was measured using cyclic voltammetry (CV). CV experiments were performed in the dry acetonitrile using $TBAPF_6$ as a supporting electrolyte (~50 mM) using a three electrode system: a Pt disc electrode as the working electrode, a Pt wire electrode as the counter electrode and Ag/Ag^+ as the reference electrode. CV of polymer film of **PNBP** coated on ITO-glass electrode in monomer free electrolyte solution showed oxidation peak at +0.52 V with onset value of 0.01 V (Figure 2.42a). The scan rate dependent CV of the **PNBP** in a monomer-free electrolyte solution indicated the formation of electro-active polymer film and there are no significant kinetic barriers to charging and discharging of

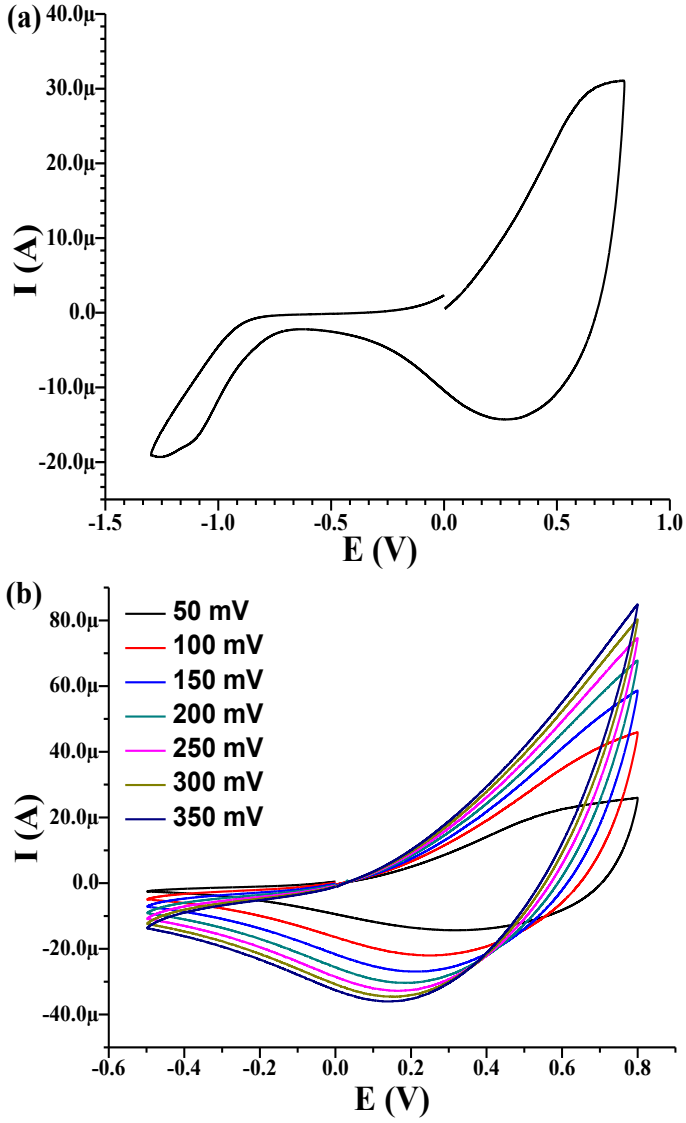

Figure 2.42 (a) Cyclic voltammogram of **PNBP** film coated on ITO-glass electrode and (b) scan rate dependence CV of the **PNBP** film coated on ITO-glass electrode, in a monomer free electrolytic solution; $E_{onset\ (Fc/Fc+)}$ = 0.36 V

the film (Figure 2.42b). The spectroelectrochemistry of polymer film on the ITO-glass electrode (Figure 2.43) showed peak at 300−415 nm and broad band at ~400−600 nm in neutral state. When oxidized by applying the potential, the high energy absorption band was gradually decreased and subsequently a broad absorption band was gradually appeared ranging from 500 nm in the visible region extending out to near IR region.

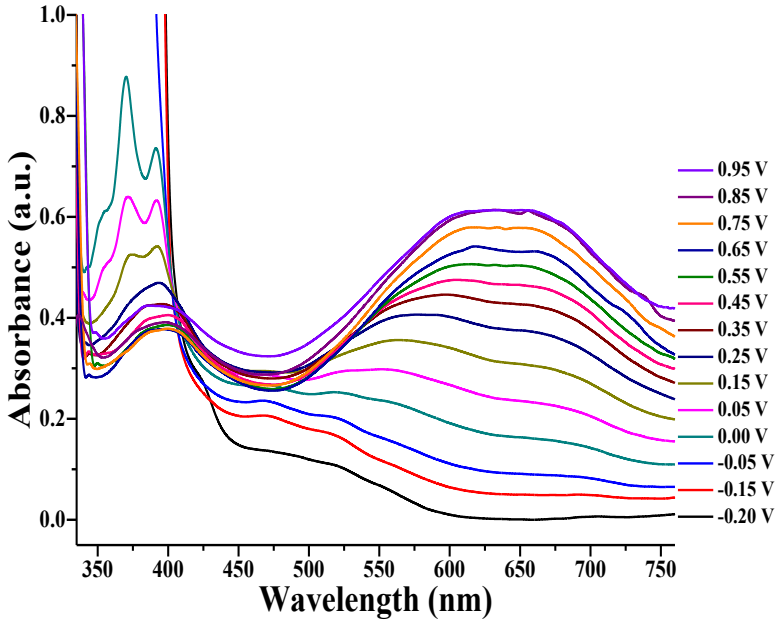

Figure 2.43 Spectroelectrochemistry of **PNBP** film coated on the ITO-electrode in a monomer free electrolytic solution

Tetracyclic fused aromatic pyrrole-based monomer **NBP** responded well to the electrochemical polymerization manifesting good α-α'-reactivity of fused pyrrole rings towards oxidative coupling compared to the tricyclic fused aromatic pyrrole-based monomers **BDP** and **DOBDP**. Therefore, **NBP** was opted as a choice of monomer for the formation of copolymer contemplating advantages like tetracyclic fused aromatic pyrrole-based structure, good β-β'-reactivity of pyrrolic positions towards electrophilic reactions and stability towards aerial oxidation.

Synthesis of copolymer PMNBP from NBP

Tetracyclic fused aromatic pyrrole-based monomer **NBP** is well-known for its predominant reactivity at carbon 3 and 8 (i.e., the β-pyrrolic positions).[28,29] The electrochemistry of **NBP** has unveiled reactivity of the α and α'-pyrrolic positions towards oxidative coupling reactions which leads to the polymer **PNBP**. To synthesize copolymer **PMNBP**, **NBP** was reacted with 3,4-(dioctyloxy)benzaldehyde in presence of $BF_3.Et_2O$; in which monomeric **NBP** units are connected by substituted methylene

bridges *via* β-position of fused-pyrroles (Scheme 3). Source of substituted methylene bridge is 3,4-(dioctyloxy)benzaldehyde, which also confers solubility to the resulting **PMNBP**.

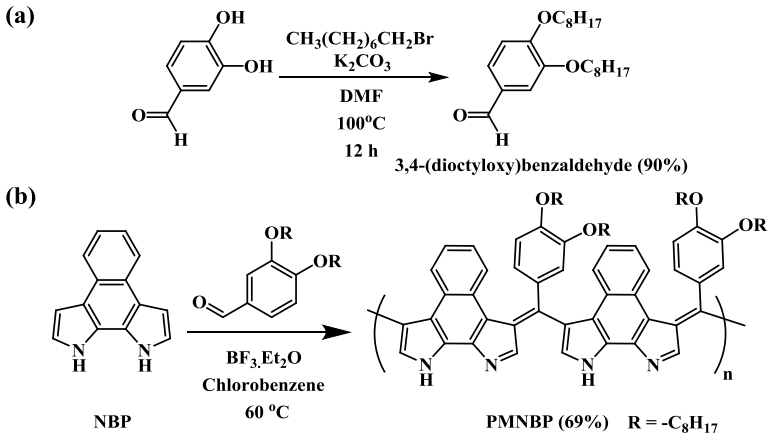

Scheme 2.4 Synthesis of (a) 3,4-(dioctyloxy)benzaldehyde from 3,4-dihydroxybenzaldehyde and (b) **PMNBP** from **NBP** and 3,4-(dioctyloxy)benzaldehyde[30]

^1H, ^{13}C NMR data and absorption spectra indicated the formation quinoidal structure through one of the pyrrole rings of naphthobipyrrole *via* air oxidation.[42] Peaks corresponding to triaryl-CH group in ^1H (δ 5.0 – 5.5 ppm) and ^{13}C (δ 50-60 ppm) NMR spectra were not observed, which indicated the formation of quinoidal structure as shown in the Scheme 2.4. It was further manifested in the absorption spectrum of PMNBP.

Thermogravimetric analysis of PMNBP

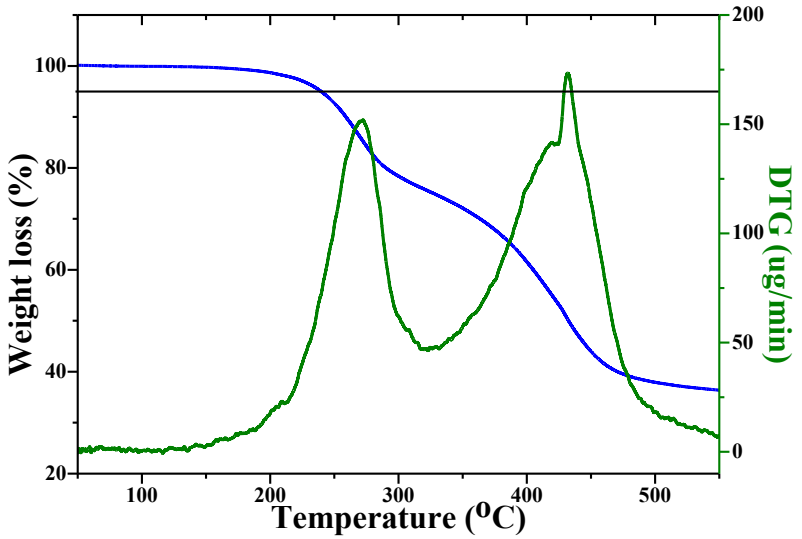

Figure 2.44 Thermogravimetric analysis of **PMNBP**; blue solid line shows TG curve and green solid line indicates DTG curve

The thermal stabilities of the synthesized polymer **PMNBP** (Figure 2.44) was investigated using thermogravimetric analysis (TGA) at the heating rate of 10 ^{o}C/min under nitrogen atmosphere. The decomposition temperature (T_d) is defined as the temperature at which the sample loses its 5% mass. **PMNBP** showed reasonable thermal stability with decomposition temperature (T_d) at 235 ^{o}C. **PMNBP** showed two step thermal degradation process which is also evident by DTG curve for **PMNBP**, however the major changes in the thermogram were observed at 250 ^{o}C and 390 ^{o}C, respectively. The observed two step degradation processes for **PMNBP** can be by virtue of the differential defragmentations of the pendant groups and the polymer backbone chain.

Molecular weight and solubility properties of PMNBP

Solubility of **PMNBP** seemed to be related directly to the structure of solubilizing alkyl/alkyl-aryl components of aldehyde. The mole ratios of aldehyde and **NBP** used during synthesis has major effect on molecular weight of resulting polymer.[43] When 1:1.05 molar ratio of aldehyde:**NBP** is used, resultant polymer has very poor solubility in most of organic solvents. When mole ratio is 1:1.15 (**NBP**:aldehyde), shorter polymer chains are formed largely, with limited molecular weight and better solubility. Therefore, for the ease of solubility and material characterization, mole ratio of 1:1.15 (**NBP**:aldehyde) is chosen which leads to less of insoluble polymers. The crude polymer **PMNBP** was further purified by soxhlet extraction using solvents of different polarities. The small oligomers and unreacted starting materials were removed by extracting the crude polymer with methanol and ethyl acetate, followed by eluting the pure fraction using chloroform. The **PMNBP** obtained from chloroform fraction showed weight average molecular weight M_w 4.8 kDa with poly-dispersity index of 1.22. The low poly-dispersity index can be attributed to the small degree of polymerization (8-9 units).

Photo-physical and conductivity properties

The optical properties of **PMNBP** were investigated using UV-vis spectroscopy. As shown in the absorption spectra (Figure 2.45a; blue solid line), **PMNBP** showed two absorption peaks in the visible region at 586 nm and 715 nm, respectively. The presence of two absorption peaks in the visible region of absorption spectra justified its intense blue color in chloroform solution, which can be ascribed to

the existence of the quinoidal form through one of the pyrrole rings of naphthobipyrrole building block along the polymeric backbone. Quinoidal form of the polymer can be formed by aerial oxidation of naphthobipyrrole-*alt*-arylmethylene copolymer. Extended conjugation and low oxidation potential of naphthobipyrrole as well as presence of *p*-alkoxy substituent on aryl ring may be the responsible factors for the formation of quinoidal polymer. Figure 2.45b shows absorption spectra of thin films of **PMNBP** (blue dashed line), casted from its chloroform solution.

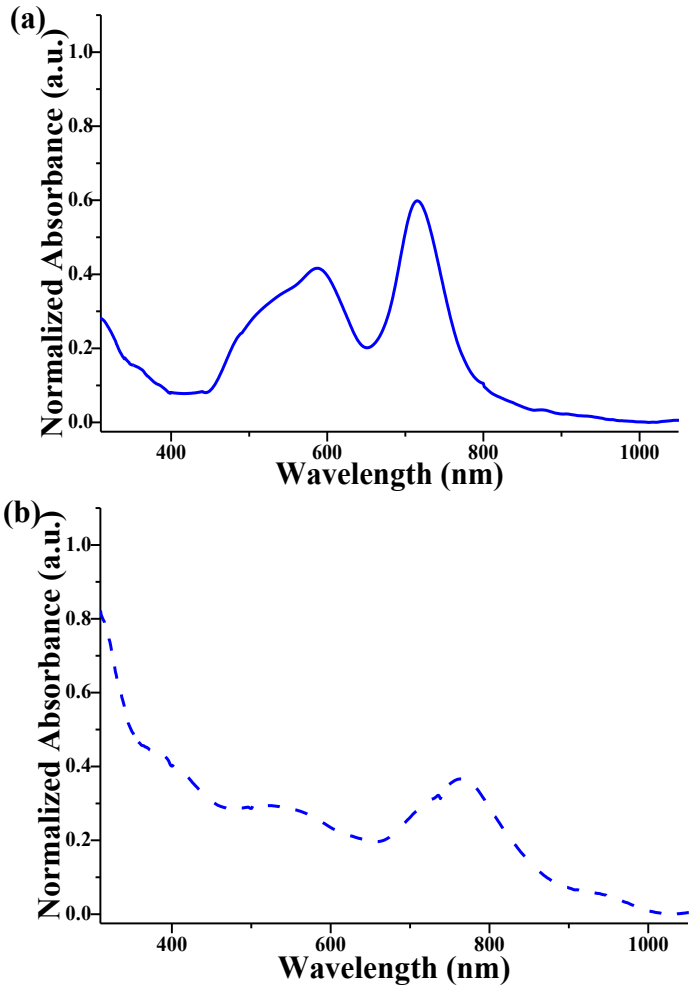

Figure 2.45 UV-Visible Spectra of (a) chloroform solution of **PMNBP** and (b) thin film of **PMNBP**

The absorption spectrum of polymer in the film state showed complex band structure with broader peaks compared to that in the solution. Due to the broadening, well defined vibronic peaks were not observed in the film state. However, bathochromic shift (~ 50 nm) was clearly observed for the peak at 715 nm which might be due to the J-type aggregation in the solid state.[44,45] Moreover, from solution to film, observed shift in the peak position indicated some kind of aggregation driven ordered chain packing in

the solid state.[46] Optical properties and optical band gaps of **PMNBP** are summarized in Table 2.2. The conductivity of **PMNBP** was measured by placing the active material between two stainless steel electrodes and waving over a frequency range of 1.2 MHz to 0.1 Hz, with 10 mV AC amplitude, at the temperature of 25 °C. The conductivity of **PMNBP** was found to be 0.124 mS cm^{-1} and the resulting electrochemical impedance spectroscopy (EIS) plot is shown in the Figure 2.46.

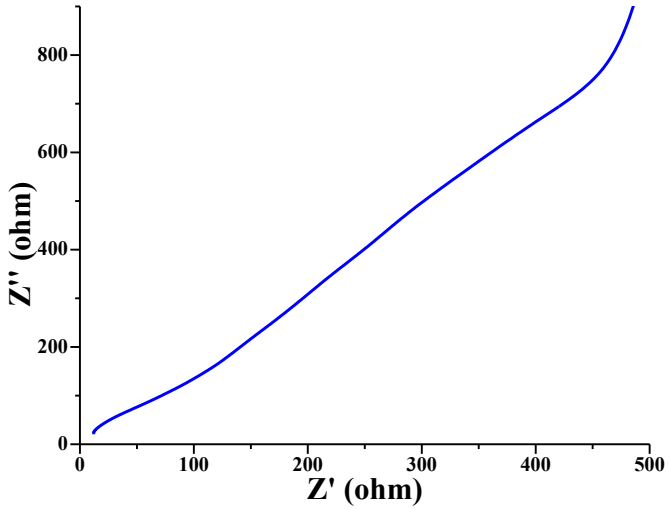

Figure 2.46 Electrochemical impedance spectroscopy (EIS) plot of **PMNBP**, The conductivity was calculated from the equation, $\sigma = {}^{l}/_{R_b A}$, where σ, R_b, *l*, and A representing conductivity (mS cm^{-1}), ohmic resistance of the bulk material, distance between the two SS electrodes and the area of the electrodes, respectively.

Electrochemical properties of polymers

The frontier orbital energy levels of the **PMNBP** were measured using cyclic voltammetry. The onset oxidation potentials and corresponding HOMO energy levels are summarized in Table 2.2. **PMNBP** showed oxidation at +0.70 V in cyclic-voltammogram (Figure 2.47a) which can be ascribed to the pyrrole-unit of the backbone. The HOMO energy level of **PMNBP** resides at −4.94 eV, respectively.

Table 2.2 Photo-physical and electrochemical properties of **PMNBP**; [a] potential v/s Ag/Ag^{+}; [b] calculated from equation $E_{HOMO} = -(E_{oxi,onset} + 4.8 - E_{onset\ (Fc/Fc+)})$; [c] calculated from equation $E_g^{el} = E_{LUMO} - E_{HOMO}$; [d] calculated using equation $E_g^{opt} = 1240/\lambda_{edge}$ (nm)

Polymer	λ_{max}^{sol} (nm)	λ_{max}^{film} (nm)	λ_{edge}^{film} (nm)	E_{oxi} [a] (V)	$E_{oxi,onset}$ [a] (V)	E_{HOMO} [b] (eV)	E_{LUMO} [c] (eV)	E_g^{opt} [d] (eV)
PMNBP	586, 715	530, 765	917	+0.70	+0.61	−4.94	−3.59	1.35

The scan rate dependent CV study of the **PMNBP** film on working Pt-disc electrode in dry acetonitrile using $TBAPF_6$ as supporting electrolyte (Figure 2.47b) showed formation of electro-active polymeric layer on the working electrode. The electro-chemical and photo-physical properties of **PMNBP** are summarized in Table 2.2.

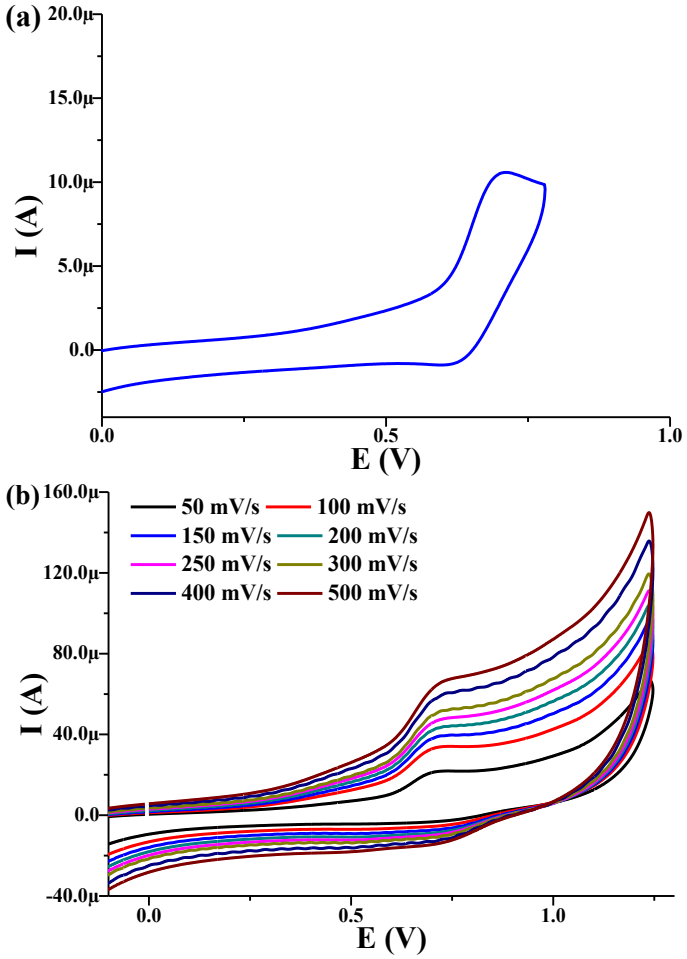

Figure 2.47 (a) Cyclic voltammogram of **PMNBP** (film casted on working electrode from chloroform solution) in dry acetonitrile using $TBAPF_6$ as a supporting electrolyte; scanned at 30 mV/s using 3-electrode system: Pt-disc electrode, Pt wire and Ag/Ag^+ reference electrode; (b) scan rate dependence of **PMNBP** film casted on Pt-disc electrode from chloroform solution in dry acetonitrile; $E_{onset\ (Fc/Fc+)}$ = 0.47 V

Conclusion

The five polycyclic fused aromatic pyrrole-based molecules **BDP**, **DOBDP**, **TOBDP**, **NBP** and **DONBP** were synthesized and their electrochemical properties were studied using cyclic voltammetry. Among these compounds, **NBP** afforded smooth polymeric film on electrochemical oxidation. The scan rate dependent CV study and electrochemical study on **PNBP** indicated its conductive and electroactive nature. Thus **NBP** was further used for the synthesis of copolymer **PMNBP**, without using any

costlier transition metal catalysts and harsh reaction conditions in terms of temperature and pressure. **PMNBP** was synthesized by reacting **NBP** with arylaldehyde, exploiting the reactivity of *β*-pyrrolic positions towards electrophilic substitution reaction. Electrochemistry, NMR and absorption spectroscopy indicated the formation of quinoidal polymer through one of the pyrrole rings of **NBP** building block.

Experimental procedures

General procedures

All the chemicals were reagent grade and used as purchased. Moisture-sensitive reactions were performed under an inert atmosphere of dry nitrogen with dried solvents. Reactions were monitored by thin-layer chromatography (TLC) analysis using Merck 60 F_{254} aluminium-coated plates and the spots were visualized under ultraviolet (UV) light. Column chromatography was carried out on silica gel (60–120 mesh). NMR spectra were recorded on a Bruker Avance-III 400 spectrometer in $CDCl_3$ and DMSO-D_6. UV-Visible absorption spectra were recorded on Jasco V-630 spectrophotometer using quartz cuvette. CV data were obtained with CH Instruments model of CHI 600C with three electrode (Pt disc/glassy carbon as the working electrode, platinum as the counter electrode, and nonaqueous $Ag/AgNO_3$ as the reference electrode) cells in anhydrous acetonitrile solution containing 50 mM tetra-*n*-butylammonium hexafluorophosphate ($TBAPF_6$) at a scan rate of 30 mV/s and 50 mV/s under an N_2 atmosphere. The redox onset potential of ferrocene/ferrocene$^+$ ($E_{onset\ (Fc/Fc+)}$) under the same conditions is recorded. The HOMO levels were calculated by using the equation: $E_{HOMO} = -(E_{oxi,onset} + 4.8 - E_{onset\ (Fc/Fc+)})$. Gel permeation chromatography was performed over Resipore/PLgel 5 µm Mixed-C column at 40 ^oC temperature, using THF as eluent at a flow rate of 1-2 mL/min taking polystyrene as a standard. Thermo-Gravimmetric Analysis (TGA) of the polymer was done on Exstar SII TG/DTA 6300 using N_2 as inert gas. The conductivity was measured using Solartron 1287 electrochemical interface and 1260 impedance gain phase analyzer interface by placing the active material between two stainless steel electrodes waving over a frequency range of 1.2 MHz to 0.1 Hz with 10 mV AC amplitude at 25 °C.

Synthesis of monomer and polymers

Synthesis of 3,4-(dioctyloxy)benzaldehyde: 3,4-(dioctyloxy)benzaldehyde was synthesized using a modification of the method reported by Elliott *et al.*[47] A mixture of 3,4-(dihydroxy)benzaldehyde (1.00 g, 7.24 mmol), *n*-octylbromide (3.49 g, 18.07 mmol), K_2CO_3 (8 g, 57.92 mmol) and few crystals of KI was dissolved in DMF (35 ml) and stirred overnight at 100 ^oC. Reaction mixture was quenched in ice cold water, neutralised with 1 M HCl solution, filtered and dried in high vacuum. The crude product was purified by column chromatography over silica gel using 10% ethyl acetate-petroleum ether as eluent. The pure product was obtained as off white solid in 90% yield.

3,4-(Dioctyloxy)benzaldehyde: Off white solid (2.36 g, 90%); ^1H NMR (400 MHz, $CDCl_3$): 9.84 (s, 1H), 7.44−7.40 (m, 2H), 6.96−6.98 (d, J = 8.0 Hz, 1H), 4.11−4.05 (m, 4H), 1.89−1.82 (m, 4H), 1.51−1.47 (m, 4H), 1.39−1.30 (m, 18H), 0.89−0.91 (t, J = 6.8 Hz, 6H). Other characterization data are according to the literature.[47]

Synthesis of **PMNBP** from **NBP**: The copolymer **PMNBP** was synthesized according to the following procedure. Monomer **NBP** (0.05 g; 0.25 mmol) was dissolved in chlorobenzene (~20 mM solution) in a clean and dry two necked round bottom flask and stirred at 0 ^oC for 5 min. The ~20 mM solution of 3,4-(dioctyloxy)benzaldehyde (0.10 g; 0.28 mmol) in chlorobenzene was taken in the addition funnel, to which $BF_3.Et_2O$ (45% solution in diethyl ether, 0.54 mL, 2.00 mmol) was added. This solution was added drop-wise to **NBP** solution at 0 ^oC and then the reaction mixture is stirred at 0 ^oC for 1 h and kept at 60 ^oC for 24 h. After completion of reaction as indicated by TLC, the reaction mixture is quenched by addition of de-ionized water and allowed to stir at room temperature for 2 h, followed by extraction with dichloromethane. The organic layer was washed multiple times with de-ionized water and finally with brine for the complete removal of HBF_4 and $B(OH)_3$. The organic layer was subjected to rotary evaporation and crude polymer obtained was subjected to soxhlet extraction to remove traces of monomers and oligomers using methanol. The **PMNBP** was eluted using chloroform. After removal of solvent, the product **PMNBP**, which is deep blue colored, was vacuum dried at 60 ^oC.

PMNBP: Deep blue-black solid (0.09 g, 69%);^{1}H NMR (400 MHz, $CDCl_3$): 9.84 (br s, N*H*), 7.85-8.14 (m, naphthalene-*H* and N=C*H*), 7.37-7.43 (m, naphthalene-*H*), 7.31-7.35 (m, Ar-*H*/NH-C*H*), 6.95-6.97 (d, J = 6.8 Hz, Ar-*H*), 4.07 (br s, O-CH_2), 1.85 (br s, O-CH_2-CH_2), 1.27-1.48 (m, -CH_2-), 0.90 (br s, -CH_3). ^{13}C NMR (100 MHz, $CDCl_3$, δ): 154.6, 149.4, 139.3, 129.8, 126.7, 125.4, 124.2, 124.1, 124.0, 123.5, 123.4, 119.1, 115.6, 114.1, 111.7, 110.8, 69.1, 33.8, 31.9, 31.8, 31.6, 29.7, 29.6, 29.3, 29.3, 29.3, 29.2, 29.2, 29.1, 29.0, 28.9, 25.9, 25.9, 22.6, 14.1. GPC (THF): Mn 3996 Dalton; Mw 4878 Dalton; PDI 1.22. IR (KBr, cm^{-1}): 3399.4, 2922.1, 2851.2, 1629.0, 1594.9, 1510.7, 1464.9, 1320.8, 1303.6, 1262.0, 1136.0, 979.9, 754.6, 675.6.

Spectral data

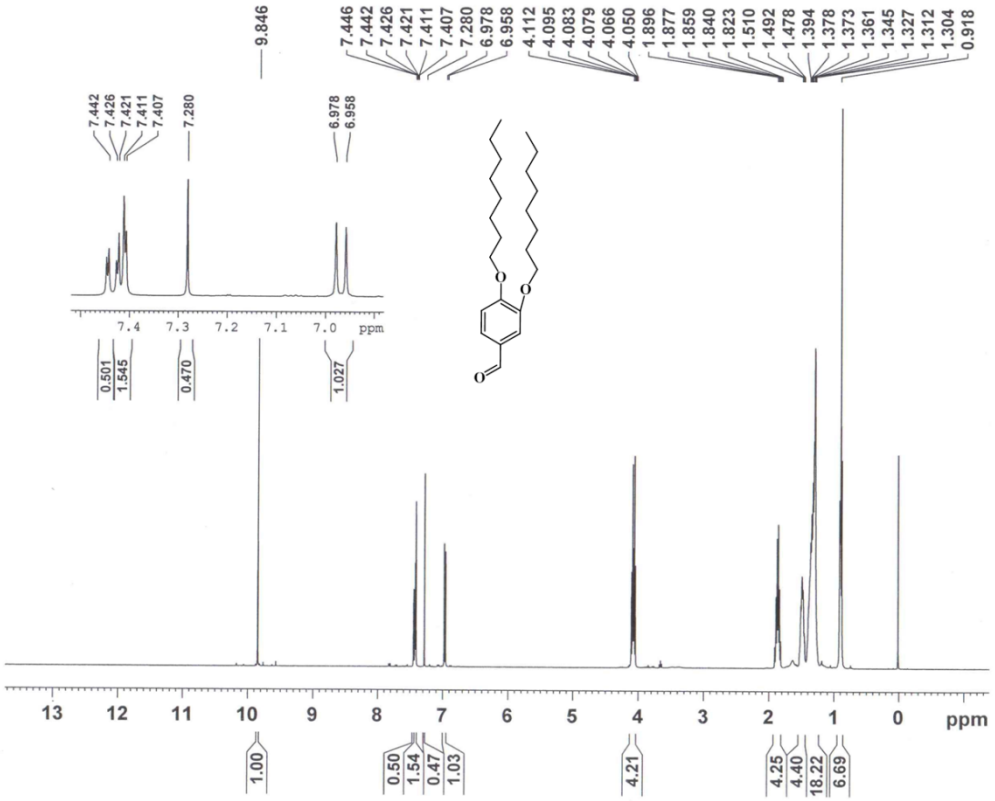

Figure 2.48 ^{1}H NMR spectrum of 3,4-(dioctyloxy)benzaldehyde

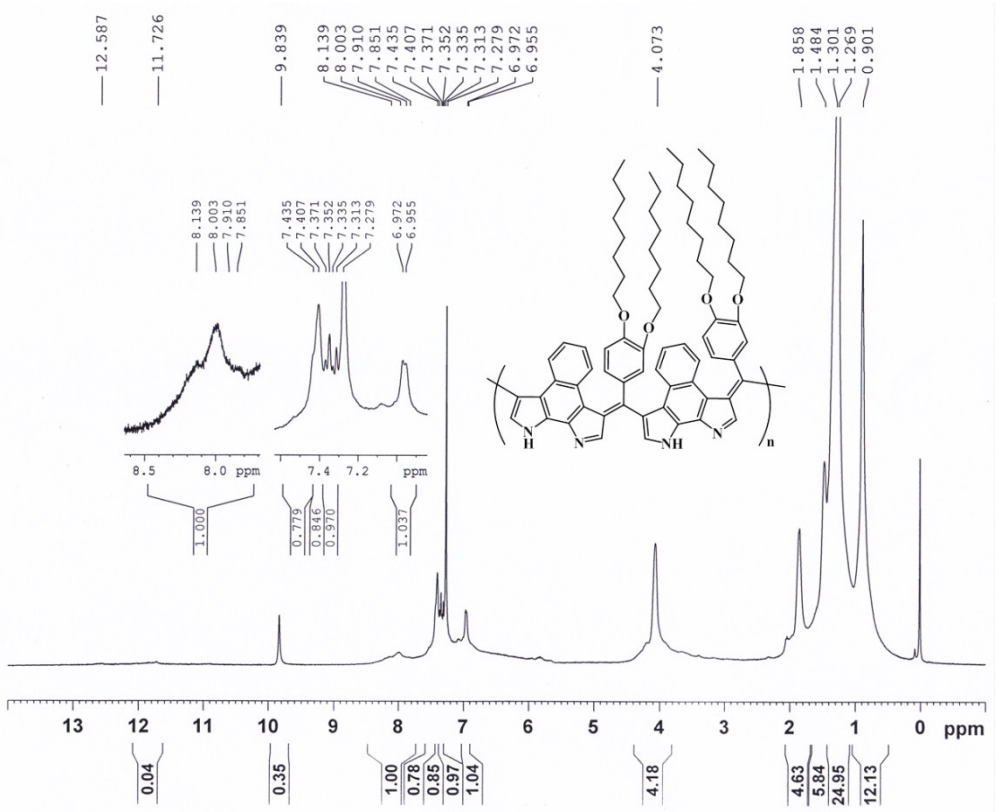

Figure 2.49 ^{1}H NMR spectrum of copolymer **PMNBP**

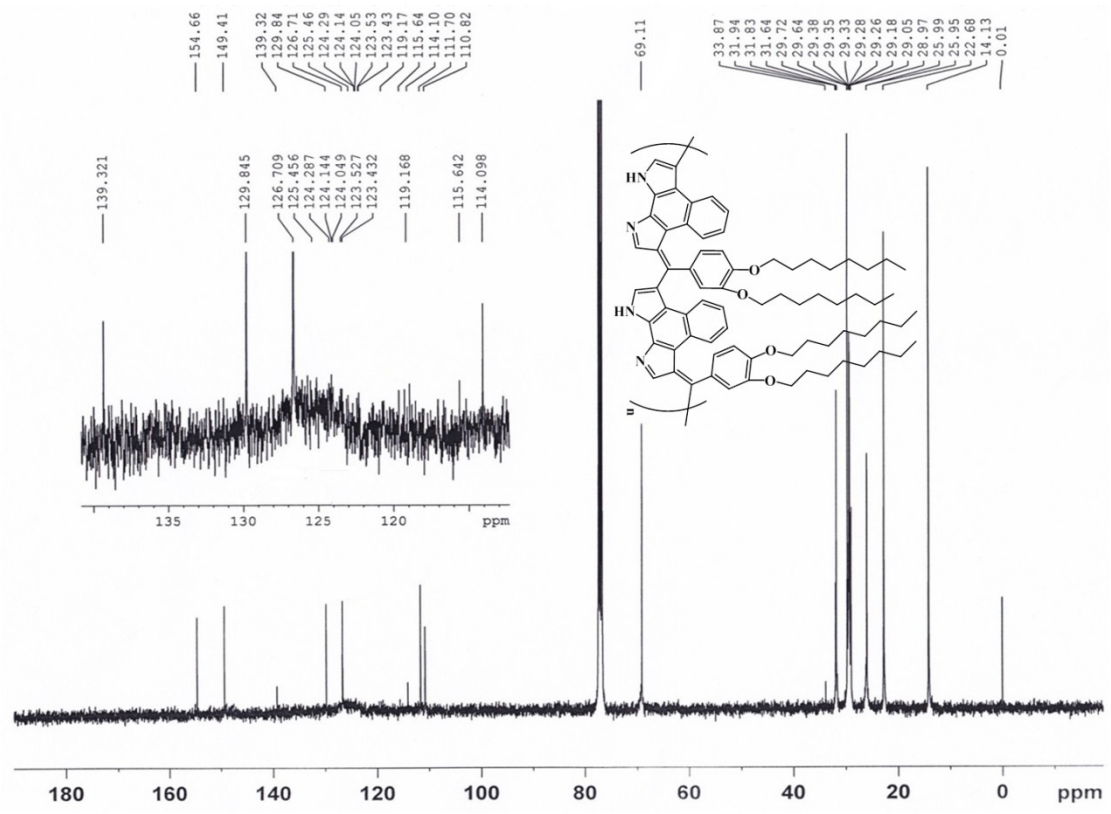

Figure 2.50 ^{13}C NMR spectrum of copolymer **PMNBP**

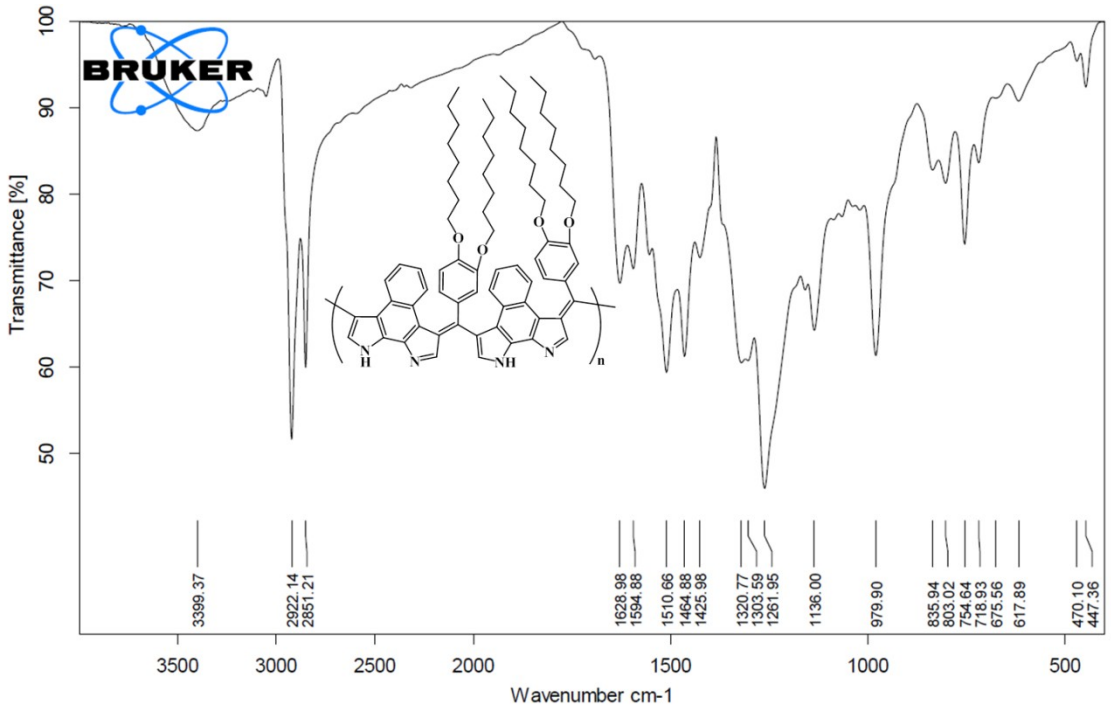

Figure 2.51 IR spectrum (KBr pellet) of **PMNBP**

GPC Result Summary

Acquired by	:PMNBP PL
Sample Name	:PMNBP PL
Sample ID	:PMNBP PL
Vail#	:64
Injection Volume	:10 µL
Data Filename	:3,4-PMNBP PL.04.lcd
Method Filename	:Polystyrene.lcm
Batch Filename	:
Report Filename	:Default.lcr

Chromatogram and Calibration Curve

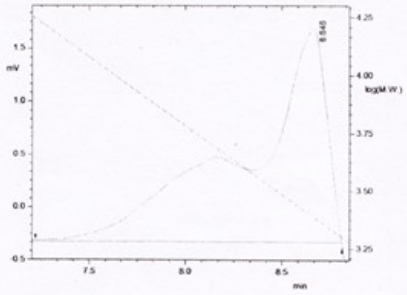

Molecular Weight Distribution Curve

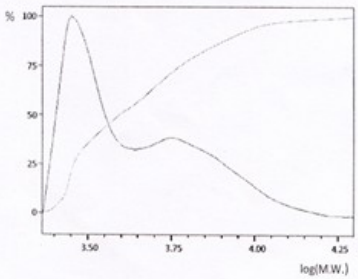

GPC Calculation Results
Peak#: 1 (Detector A Ch1)
[Peak Information]

	Time (min)	Volume (mL)	Molecular Weight	Height
Start	7.308	7.308	19054	-338
Top	8.646	8.646	2857	2126
End	8.808	8.808	2269	-334

Area	: 58361
Area %	:100.0000

[Average Molecular Weight]

Number Average Molecular Weight(Mn)	3996
Weight Average Molecular Weight(Mw)	4878
Z Average Molecular Weight(Mz)	6152
Z+1 Average Molecular Weight(Mz1)	7612
Mw/Mn	1.22072
Mv/Mn	0.00000
Mz/Mw	1.26117

D:¥MSU¥Arun¥3,4-PMNBP PL04.lcd

Figure 2.52 Gel Permeation Chromatography report of copolymer **PMNBP**

References

1 F. Garnier, R. Hajlaoui, A. Yassar and P. Srivastava, *Science*, 1994, **265**, 1684–1686.

2 H. Sirringhaus, N. Tessler and R. H. Friend, *Science*, 1998, **280**, 1741–1744.

3 J. Liu, R. Zhang, G. Sauvé, T. Kowalewski and R. D. McCullough, *J. Am. Chem. Soc.*, 2008, **130**, 13167–13176.

4 D.-K. Moon, A. B. Padias, H. K. Hall, T. Huntoon and P. D. Calvert, *Macromolecules*, 1995, **28**, 6205–6210.

5 D. M. Ivory, G. G. Miller, J. M. Sowa, L. W. Shacklette, R. R. Chance and R. H. Baughman, *J. Chem. Phys.*, 1979, **71**, 1506–1507.

6 A. Abdulkarim, F. Hinkel, D. Jänsch, J. Freudenberg, F. E. Golling and K. Müllen, *J. Am. Chem. Soc.*, 2016, **138**, 16208–16211.

7 K. Friedrich, H. J. Sue, P. Liu and A. A. Almajid, *Tribol. Int.*, 2011, **44**, 1032–1046.

8 Z. A. Boeva and V. G. Sergeyev, *Polym. Sci. Ser. C*, 2014, **56**, 144–153.

9 H. Wang, J. Lin and Z. X. Shen, *J. Sci. Adv. Mater. Devices*, 2016, **1**, 225–255.

10 S. Bhadra, D. Khastgir, N. K. Singha and J. H. Lee, *Prog. Polym. Sci.*, 2009, **34**, 783–810.

11 C. H. B. Silva, N. A. Galiote, F. Huguenin, É. Teixeira-Neto, V. R. L. Constantino and M. L. A. Temperini, *J. Mater. Chem.*, 2012, **22**, 14052–14060.

12 T. P. Kaloni, P. K. Giesbrecht, G. Schreckenbach and M. S. Freund, *Chem. Mater.*, 2017, **29**, 10248–10283.

13 R. Ferro, A. Besostri, A. Olivieri and E. Stellini, *Eur. J. Paediatr. Dent.*, 2016, **17**, 36–42.

14 T. A. Skotheim, *Handbook of Conducting Polymers, Volume 1*, Marcel Dekker Inc., New York, 1986.

15 T. A. Skotheim, *Handbook of Conducting Polymers, Volume 2*, Marcel Dekker Inc., New York, 1986.

16 T. A. Skotheim, R. L. Elsenbaumer and J. R. Reynolds, *Handbook of Conducting Polymers*, Marcel Dekker Inc., New York, Second Edi., 1998.

17 G. G. Wallace, G. M. Sprinks and P. R. Teasdale, *Conductive Electroactive Polymers: Intelligent Materials Systems*, Technomic, Lancaster, Second Edi., 1997.

18 L.-X. Wang, X.-G. Li and Y.-L. Yang, *React. Funct. Polym.*, 2001, **47**, 125–139.

19 M. R. Bryce, A. Chissel, P. Kathirgamanathan, D. Parker and N. R. M. Smith, *J. Chem. Soc. Chem. Commun.*, 1987, 466–467.

20 G. A. Sotzing, J. R. Reynolds, A. R. Katritzky, J. Soloducho, S. Belyakov and R. Musgrave, *Macromolecules*, 1996, **29**, 1679–1684.

21 T. Y. Wu, J. W. Liao and C. Y. Chen, *Electrochim. Acta*, 2014, **150**, 245–262.

22 J. M. Nadeau and T. M. Swager, *Tetrahedron*, 2004, **60**, 7141–7146.

23 S. I. Kato, T. Furuya, A. Kobayashi, M. Nitani, Y. Ie, Y. Aso, T. Yoshihara, S. Tobita and Y. Nakamura, *J. Org. Chem.*, 2012, **77**, 7595–7606.

24 M. Heeney, C. Bailey, K. Genevicius, M. Shkunov, D. Sparrowe, S. Tierney and I. McCulloch, *J. Am. Chem. Soc.*, 2005, **127**, 1078–1079.

25 I. McCulloch, M. Heeney, C. Bailey, K. Genevicius, I. MacDonald, M. Shkunov, D. Sparrowe, S. Tierney, R. Wagner, W. Zhang, M. L. Chabinyc, R. J. Kline, M. D. McGehee and M. F. Toney, *Nat. Mater.*, 2006, **5**, 328–333.

26 P. Coppo and M. L. Turner, *J. Mater. Chem.*, 2005, **15**, 1123.

27 G. R. Hutchison, M. A. Ratner and T. J. Marks, *J. Am. Chem. Soc.*, 2005, **127**, 2339–2350.

28 M. V Trapaidze, S. A. Samsoniya, N. A. Kuprashvili, L. M. Mamaladze and N. N. Suvorov, *Khim. Geterotsikl. Soedin.*, 1988, 603–609.

29 S. A. Samsoniya, M. V. Trapaidze and N. A. Kuprashvili, *Pharm. Chem. J.*, 2009, **43**, 92–94.

30 V. J. Bhanvadia, Y. J. Mankad, A. L. Patel and S. S. Zade, *New J. Chem.*, 2018, **42**, 13565–13572.

31 A. Berlin, S. Bradamante, R. Ferraccioli, G. A. Pagani and F. Sannicolo, *J. Chem. Soc. Chem. Commun.*, 1987, 1176–1177.

32 G. K. B. Clentsmith, L. D. Field, B. A. Messerle, A. Shasha and P. Turner, *Tetrahedron Lett.*, 2009, **50**, 1469–1471.

33 B. A. D. Neto, A. S. Lopes, G. Ebeling, R. S. Goncalves, V. E. U. Costa, F. H. Quina and J. Dupont, *Tetrahedron*, 2005, **61**, 10975–10982.

34 A. L. Appleton, S. Miao, S. M. Brombosz, N. J. Berger, S. Barlow, S. R. Marder, B. M. Lawrence, K. I. Hardcastle and U. H. F. Bunz, *Org. Lett.*, 2009, **11**, 5222–5225.

35 B. D. Lindner, B. A. Coombs, M. Schaffroth, J. U. Engelhart, O. Tverskoy, F. Rominger, M. Hamburger and U. H. F. Bunz, *Org. Lett.*, 2013, **15**, 666–669.

36 A. Yasuhara, Y. Kanamori, M. Kaneko, A. Numata, Y. Kondo and T. Sakamoto, *J. Chem. Soc., Perkin Trans. 1*, 1999, 529–534.

37 S. A. Samsoniya, M. V Trapaidze, N. A. Kuprashvili, A. M. Kolesnikov and N. N. Suvorov, *Khim. Geterotsikl. Soedin.*, 1985, 1222–1224.

38 V. Roznyatovskiy, V. Lynch and J. L. Sessler, *Org. Lett.*, 2010, **12**, 4424–4427.

39 H. Franzen, *J. Prakt. Chem.*, 1908, **76**, 205.

40 H. Franzen, *J. für Prakt. Chemie*, 1907, **76**, 205–232.

41 A. F. Diaz, J. Crowley, J. Bargon, G. P. Gardini and J. B. Torrance, *J. Electroanal. Chem.*, 1981, **121**, 355–361.

42 C. C. Silveira, S. R. Mendes, M. A. Villetti, D. F. Back and T. S. Kaufman, *Green Chem.*, 2012, **14**, 2912–2921.

43 J. J. Intemann, K. Yao, H. Yip, Y. Xu, Y. Li, P. Liang, F. Ding, X. Li and A. K. Jen, *Chem. Mater.*, 2013, **25**, 3188–3195.

44 H. Hwang, D. Khim, J. M. Yun, E. Jung, S. Y. Jang, Y. H. Jang, Y. Y. Noh and D. Y. Kim, *Adv. Funct. Mater.*, 2015, **25**, 1146–1156.

45 J. M. W. Chan, J. R. Tischler, S. E. Kooi, V. Bulovic and T. M. Swager, *J. Am. Chem. Soc.*, 2009, **131**, 5659–5666.

46 Y. Deng, B. Sun, Y. He, J. Quinn, C. Guo and Y. Li, *Angew. Chemie - Int. Ed.*, 2016, **55**, 3459–3462.

47 J. M. Elliott, J. R. Chipperfield, S. Clark and E. Sinn, *Inorg. Chem.*, 2001, **40**, 6390–6396.